MARMARA UNIVERSITY
FACULTY OF ENGINEERING

MECHANICAL ENGINEERING DEPARTMENT

IMPROVING THE MECHANICAL STRENGTH IN THERMOSETTING LAMINATES USING ELECTROSPUN FIBERS

Amirmohammad MOTTAGHINIA, Enes AKYOL, Rikesh POKHAREL

GRADUATION PROJECT

Department of Mechanical Engineering

Supervisor

Prof. Dr. Paşa YAYLA

ISTANBUL, 2025

MARMARA UNIVERSITY
FACULTY OF ENGINEERING

MECHANICAL ENGINEERING DEPARTMENT

IMPROVING THE MECHANICAL STRENGTH IN THERMOSETTING LAMINATES USING ELECTROSPUN FIBERS

by

Amirmohammad MOTTAGHINIA, Enes AKYOL, Rikesh POKHAREL

July 2025, ISTANBUL

SUBMITTED TO THE DEPARTMENT OF MECHANICAL ENGINEERING IN PARTIAL FULFILLMENT OF THE REQUIREMENTS FOR THE DEGREE OF BACHELOR OF SCIENCE AT MARMARA UNIVERSITY

Signature of Author(s) .....

Department of Mechanical Engineering

Certified By .....

Project Supervisor, Department of Mechanical Engineering

Accepted By.....

Head of the Department of Mechanical Engineering

ACKNOWLEDGEMENT

First of all, we would like to thank our supervisor Prof. Dr. Paşa YAYLA for the valuable guidance and advice on preparing this thesis and giving us moral and material support.

We are very grateful to Asst. Prof. Muhammet CEYLAN for allowing us to use his laboratory and equipment at Istanbul Ticaret University.

We would like to express our gratitude to Prof. Dr. Erhan SANCAK for allowing us to use his heat press laboratory and equipment at Marmara University.

We would like to express our gratitude to Prof. Dr. Cevat SARIOGLU for allowing us to use his laboratory and equipment at Marmara University.

Amirmohammad MOTTAGHINIA
, Enes AKYOL
Rikesh POKHAREL

June, 2025

CONTENTS

ÖZET

Bu bitirme projesinde, termoset laminatların mekanik dayanımını artırmak amacıyla elektrospin yöntemiyle üretilmiş nanoliflerin kullanımı incelenmiştir. Karbon fiber ve epoksi esaslı kompozit laminatlar arasına yerleştirilen polikaprolakton (PCL) esaslı elektrospin lifler, arayüz bağlanmasını iyileştirerek çatlak yayılımını önlemekte ve delaminasyonu azaltmaktadır. Bu yöntem sayesinde, kompozit yapıların darbe dayanımı, çekme mukavemeti ve enerji sönümleme kapasitesi anlamlı şekilde artırılmıştır.

Proje kapsamında önce elektrospin parametreleri optimize edilerek homojen PCL nanolif matları üretilmiş, ardından bu lifler kompozit katmanlar arasında yerleştirilerek sıcak pres yöntemiyle numuneler hazırlanmıştır. Hazırlanan numuneler üzerinde çekme ve Charpy darbe testleri gerçekleştirilmiş ve elektrospin lif içeren numunelerin, lif içermeyenlere kıyasla daha yüksek tokluk ve enerji absorpsiyon kapasitesine sahip olduğu gözlemlenmiştir. Ayrıca, fiber yönelimi ve üretim sürecinin nihai mekanik performans üzerindeki etkisi de detaylı şekilde analiz edilmiştir.

Sonuç olarak, elektrospin yöntemiyle elde edilen nanoliflerin termoset kompozit laminatların zayıf yönlerinden biri olan kırılgan yapısını önemli ölçüde iyileştirdiği gösterilmiştir. Bu çalışma, ileri düzey yapısal uygulamalarda kullanılabilecek daha dayanıklı ve güvenilir kompozit malzemelerin geliştirilmesine katkı sağlamaktadır.

ABSTRACT

Thermosetting laminates, known for their high strength to weight ratio and thermal resistance, are widely utilized in aerospace, automotive, and industrial applications. However, their inherent brittleness and susceptibility to interlaminar delamination limit their performance under high-stress conditions. To address these challenges, electrospinning was employed to fabricate core-shell nanofibers composed of Polycaprolactone (PCL) and epoxy. These nanofibers were incorporated as interleaves in carbon fiber/epoxy composite laminates to improve interfacial bonding and mechanical toughness. Comprehensive mechanical testing, including tensile strength, flexural strength, interlaminar fracture toughness, and interlaminar shear strength evaluations, revealed significant improvements in the modified laminates. The results indicate that the inclusion of electrospun nanofiber interleaves enhances stress distribution, mitigates delamination, and increases energy absorption capacity. This approach demonstrates the potential of electrospun fibers as a viable method for optimizing the mechanical performance of thermosetting laminates, contributing to the development of advanced composite materials for high performance applications.

Keywords: nanofibers; electrospun; electrospinning; mechanical properties; epoxy; resin; thermosetting laminates; cohesive failure; matrix; tensile;

SYMBOLS

mm: Millimeter

µm: Micrometer

g: Gram

g/cm3: Gram per cubic centimeter

kN: Kilonewton

B: Width

t: Thickness

A: Cross-sectional Area

σ: Stress

σut: Ultimate tensile strength

ε: Strain

εut: Ultimate tensile strain

Fmax: Max force

δmax: Maximum displacement

Lg: Gage length

E: Elastic Modulus

CVN: Charpy Impact Strength

GPa: Gigapascal

Mpa: Megapascal

ABBREVIATIONS

PCL: Polycaprolactone

DMF: Dimethylformamide

UTS: Ultimate Tensile Strength

CVN: Charpy V-Notch

CFRP: Carbon Fiber Reinforced Polymer

CLT: Classical Laminate Theory

PAN: Polyacrylonitrile

CNT: Carbon Nanotube

NBR: Nitrile Butadiene Rubber

ASTM: American Society for Testing and Materials

TCD: Tip to Collector Distance

DC: Direct Current

LIST OF FIGURES

LIST OF TABLES

1. INTRODUCTION

Composite materials have revolutionized modern engineering and manufacturing, offering a combination of properties that surpass those of their individual components. By merging materials with distinct characteristics, composites provide lightweight, high-strength, and versatile solutions for industries such as aerospace, automotive, and construction. Among the different types of composites, thermosetting laminates stand out due to their superior performance under extreme conditions. These materials are created by combining thermosetting resins with reinforcing fibers to achieve exceptional mechanical strength, thermal resistance, and chemical stability. Their adaptability allows them to be tailored to specific industrial needs, making them indispensable in various high-performance applications.

Thermosetting epoxy, a widely used resin, is a two-part polymer system composed of an epoxide resin and a curing agent. This combination undergoes an irreversible chemical reaction, forming a rigid, crosslinked structure that imparts remarkable properties such as durability, adhesion, and resistance to heat, chemicals, and moisture. However, epoxy resins also have limitations, primarily their brittleness and susceptibility to cohesive failure under high stress or impact conditions. These failures occur internally within the epoxy matrix, leading to cracks and fractures that can compromise the integrity of the entire structure. To mitigate these shortcomings, researchers and engineers continually explore methods to enhance the mechanical toughness of epoxy-based systems.

Thermosetting laminates are composite structures formed by layering reinforcing fibers, such as carbon or glass fibers, with thermosetting resins like epoxy, polyester, or phenolic resins. The curing process involves the application of heat and pressure, triggering crosslinking in the resin matrix, which bonds the layers into a unified, rigid material. These laminates are particularly valued for their high strength-to-weight ratio, excellent thermal insulation, and resistance to environmental degradation. They are extensively used in aerospace and automotive industries to reduce vehicle weight while maintaining structural integrity, ultimately improving fuel efficiency and performance. Despite their advantages, the brittle nature of thermosetting resins can lead to

cohesive failures in high-stress scenarios. As such, optimizing the mechanical performance and failure resistance of these materials remains a priority.

One promising solution to improve the mechanical properties of thermosetting laminates lies in the integration of electrospun fibers. Electrospinning is a highly versatile and efficient technique for producing nanofibers with exceptional properties. By applying a high-voltage electric field to a polymer solution or melt, continuous ultrafine fibers with diameters ranging from nanometers to micrometers can be generated. These fibers offer a high surface area-to-volume ratio, tunable porosity, and outstanding mechanical strength, making them ideal for applications such as reinforcement in composites, filtration, tissue engineering, and energy storage. In composite laminates, electrospun fibers enhance interfacial bonding, distribute stress more evenly, and improve resistance to cracking and delamination.

The flexibility of electrospinning technology allows for customization of fiber properties to suit specific applications. Traditional needle-based electrospinning offers precision in fiber morphology, while advanced techniques like coaxial electrospinning enable the production of core-shell fibers with distinct internal and external layers. These innovations have broadened the scope of electrospinning, enabling the development of hybrid materials with tailored mechanical, thermal, and functional properties. For example, incorporating electrospun nanofibers with thermosetting laminates significantly enhances toughness, ductility, and fracture resistance, thereby addressing the limitations of brittle resin systems.

The integration of electrospinning and thermosetting laminates represents a frontier in material science. By combining the lightweight strength of laminates with the enhanced toughness provided by nanofiber reinforcement, engineers can develop composites with unprecedented performance characteristics. This report delves into the critical aspects of thermosetting epoxy, laminates, and electrospinning, exploring their roles in advancing composite materials for modern engineering challenges. The significance of these technologies, their mechanisms of action, and their potential to transform material applications are analyzed in detail, providing a comprehensive understanding of their contributions to the field.

2. Background and Literature Survey

2.1 Composite Materials

Composite materials are engineered systems composed of two or more constituent phases with markedly different physical, chemical, and mechanical characteristics. When combined at the macroscopic level, these constituents produce a material with enhanced performance properties that surpass those of the individual components. This synergistic behavior allows composites to exhibit superior attributes such as high specific strength and stiffness, enhanced wear and corrosion resistance, reduced weight, improved thermal and electrical conductivity, extended fatigue life, and excellent thermal insulation capabilities. As a result, composite materials have become increasingly prevalent in a wide range of industrial applications, including aerospace, automotive, construction, electronics, and biomedical engineering.

Structurally, a composite is typically composed of a continuous matrix phase**,** which serves as the binder and stress-transfer medium, and a dispersed reinforcement phase**,** which provides strength, stiffness, and other functional properties. The reinforcement is often in the form of fibers, particles, or flakes and is embedded within the matrix to form a unified material system in Figure 2.1 [1].

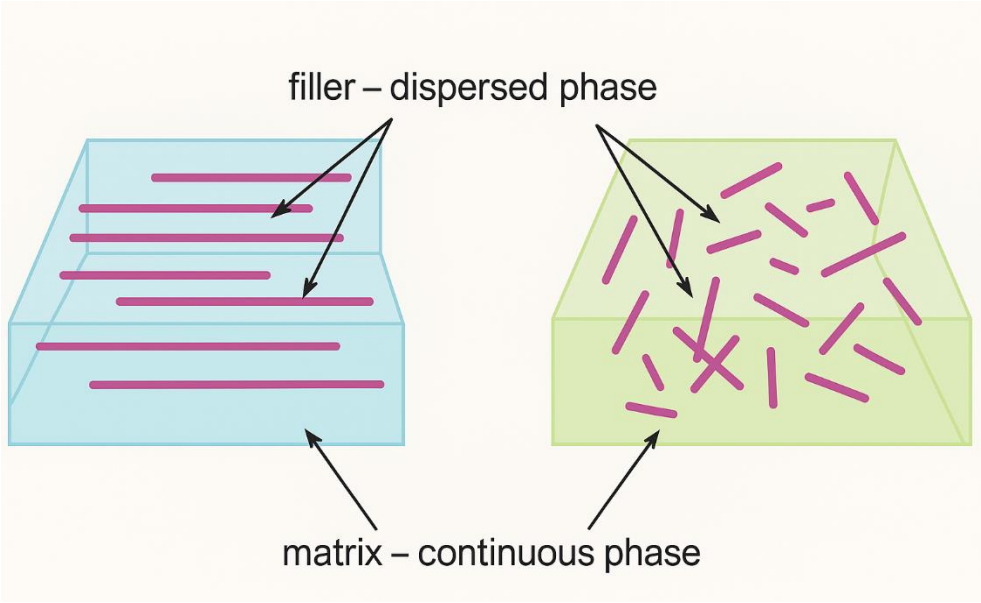

Figure 2.1: *Phases of Composites*

The matrix phase functions as a binding material. It must form a continuous structure to support and shield the filler phase from environmental factors such as moisture and chemicals. Additionally, it plays a key role in transmitting stress to the filler materials. Typically, the filler phase exhibits greater density, strength, and stiffness compared to the matrix, thereby contributing to the overall strength of the composite structure [2]. Furthermore, reinforcements enhance various composite properties, including thermal expansion coefficient and conductivity.

2.1.1 Classification of Composite Materials

Composite materials can be classified through various approaches; however, the most widely accepted and commonly utilized method of categorization is based on the nature of their matrix and reinforcement constituents, as illustrated in Figure 2.2. This classification framework enables a systematic understanding of the material's composition and mechanical behavior. According to the type of matrix phase employed, composites are broadly divided into three principal categories: Polymer Matrix Composites (PMCs), Metal Matrix Composites (MMCs), and Ceramic Matrix Composites (CMCs). Each class exhibits distinct physical, thermal, and mechanical characteristics influenced primarily by the intrinsic properties of the matrix material.

Polymer matrix composites are typically favored for their low density, ease of processing, and cost-effectiveness, making them suitable for a wide range of structural and non-structural applications. Metal matrix composites, on the other hand, are chosen for applications demanding higher thermal stability, strength, and wear resistance. Ceramic matrix composites provide superior performance in high-temperature and corrosive environments due to their inherent thermal and chemical stability.

In addition to matrix-based classification, composite materials are further distinguished based on the form and distribution of the reinforcement phase. The reinforcement can exist in various morphologies, leading to the categorization of composites into fiber-reinforced composites, particle-reinforced composites, and structural composites. Fiber-reinforced composites utilize continuous or discontinuous fibers to significantly enhance mechanical properties such as tensile strength and stiffness. Particle-reinforced composites incorporate fine particles to improve wear resistance, hardness, and dimensional stability. Structural composites,

which often involve complex architectures such as laminates or sandwich panels, are designed to meet specific mechanical and structural requirements in advanced engineering applications.

This dual classification based on both matrix and reinforcement phases provides a comprehensive framework for selecting and engineering composite materials tailored to specific performance demands and environmental conditions.

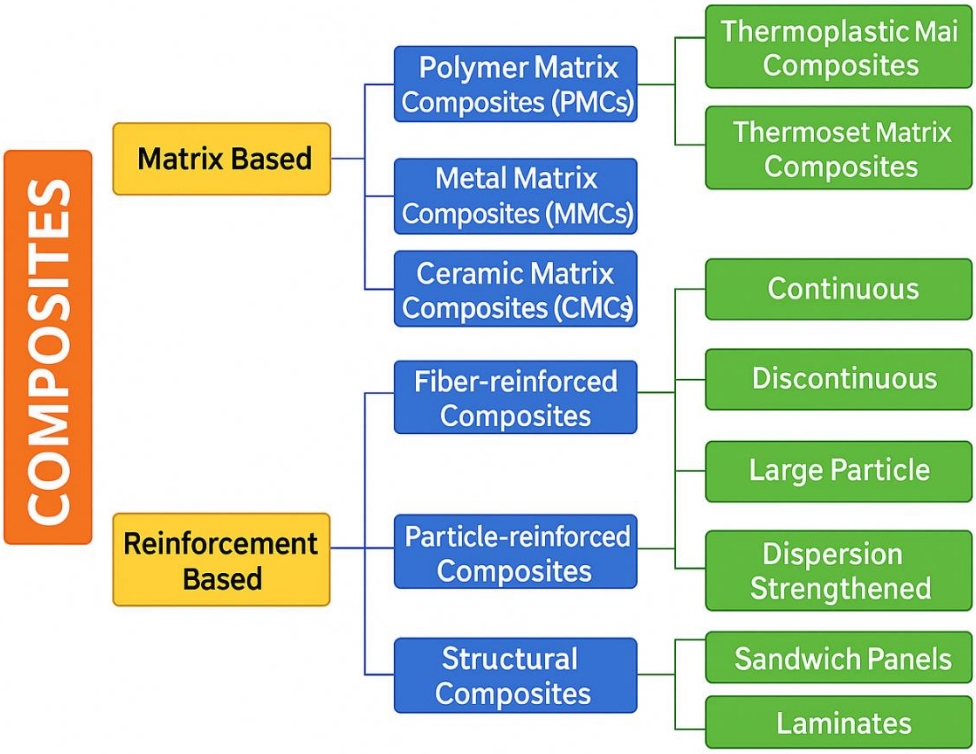

Figure 2.2: *Classifications of composites based on matrix and reinforcement.*

The selection of matrix and filler (reinforcement) phases in composite materials is primarily guided by the intended performance requirements and the specific service conditions under which the composite will operate. Key factors such as mechanical strength, thermal stability, chemical resistance, weight constraints, and cost-effectiveness play crucial roles in determining the most suitable combination of constituents. The matrix serves as the continuous phase that binds the reinforcement, distributes loads, and provides environmental protection, while the reinforcement enhances the overall structural and functional properties of the composite.

Depending on the application whether in aerospace, automotive, biomedical, or civil engineering the type of matrix (polymer, metal, or ceramic) and the nature of the reinforcement

(fibers, particles, or structural forms) can vary significantly. A strategic pairing of these components allows for the design of materials tailored to meet complex engineering demands.

A general overview of common composite types along with their representative application areas is provided in **Table 2.1**, highlighting the versatility and broad industrial relevance of composite materials across multiple sectors.

Table 2.1 : *Composite types, their properties and applications.*

Category	Type	Properties	Application area
Matrix	**Ceramic**	Low density, superior high-temperature strength, excellent creep and oxidation resistance	Structural components in civil aviation, thermal barrier coatings
	Metal	High thermal and electrical conductivity, good wear and corrosion resistance, elevated strength	Automotive components, marine structures, aerospace structural elements
	Polymer	Lightweight, high specific strength, corrosion resistance, ease of processing	Wind turbine blades, aerospace structures, biomedical devices, rocket components
Reinforcement	**Fiber**	High tensile strength and stiffness, low density, excellent thermal and chemical stability	Aerospace and aircraft components, marine parts, sports equipment, automotive body panels
	Particle	High hardness, isotropic strengthening, improved wear and fracture resistance	Construction materials, dental prosthetics, cutting tools
	Structural	High energy absorption capacity, excellent stiffness-to-weight ratio	Load-bearing components in automotive, aerospace, marine and civil engineering applications

2.1.2 Advantages and Disadvantages of Composites

Despite the numerous advantages that composite materials offer over conventional engineering materials, they also possess certain limitations that must be taken into account during material selection and design processes. While composites are highly valued for their excellent strength-to-weight ratio, corrosion resistance, design flexibility, and tailored mechanical properties, they may also exhibit disadvantages such as higher production costs, complex fabrication processes, limited

recyclability, and challenges in inspection and repair. These factors can influence their applicability in various industries depending on specific functional and economic requirements. A comprehensive overview of the primary benefits and drawbacks associated with composite materials is presented in **Table 2.2**, adapted from [3].

Table 2.2: *Advantages and disadvantages of composites*

Advantages	Disadvantages
High specific strength and low density	Relatively high production and raw material costs
Flexibility in design and manufacturing customizable to meet specific performance requirements	Difficult to repair or rework once damaged
Excellent resistance to corrosion and aggressive chemical environments	Susceptibility to ultraviolet (UV) degradation in some polymer-based composites
Superior fatigue performance under cyclic loading conditions	Inadequate recycling infrastructure and end of life management
Tailorable properties such as stiffness, thermal stability, and impact resistance	Surface finishing and appearance may not meet all aesthetic or functional standards

2.1.3 Laminates of Composites

Composite laminates have garnered increasing attention and widespread utilization across numerous high-performance engineering sectors, including the aerospace, marine, automotive, and sporting goods industries, as well as in various structural and functional applications. Among the various types of composite laminates**,** carbon fiber reinforced plastic (CFRP) laminates have emerged as a prominent material class due to their exceptional mechanical performance, superior strength-to-weight ratio, dimensional stability, and fatigue resistance [3]. These attributes make them particularly well-suited for applications requiring lightweight yet highly durable materials.

A significant proportion of such laminates are manufactured using pre-impregnated fiber materials**,** commonly referred to as prepregs**,** which consist of continuous fiber reinforcements pre-coated with a partially cured polymer resin system. This semi-cured state facilitates ease of handling and storage while ensuring uniform resin distribution throughout the laminate structure. The use of prepregs enhances the reliability and quality of the final composite, enabling precise control over fiber orientation, resin content, and laminate thickness. An illustration of a typical prepreg configuration is presented in Figure 2.3**.**

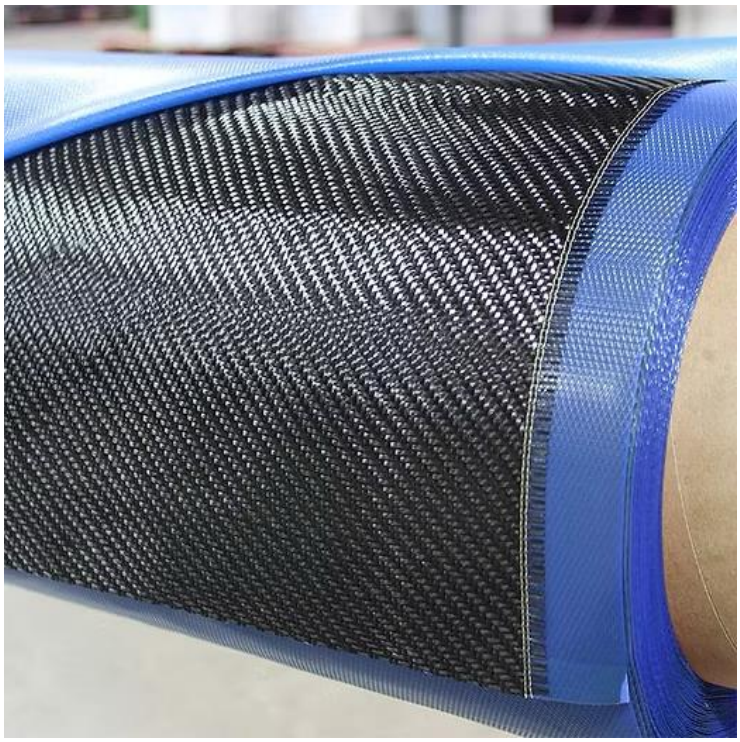

Figure 2.3: *Carbon fiber prepreg.*

Prepreg materials typically consist of a combination of continuous fiber reinforcement embedded within a highly viscous polymer matrix, most commonly epoxy resin. These pre-impregnated systems are available in two principal forms**:** unidirectional (UD)**,** where fibers are aligned in a single direction to maximize stiffness and strength along that axis, and woven fabric, which includes reinforcements oriented in multiple directions to provide balanced mechanical performance. To facilitate handling and storage, the resin matrix in prepregs is partially cured a stage often referred to as the B-stage and must be refrigerated to prevent premature

polymerization. Full polymerization and consolidation of the laminate are achieved through the application of elevated temperature and pressure during the curing cycle [4].

Composite laminates can be tailored to exhibit specific mechanical and thermal characteristics such as stiffness, tensile strength, and thermal stability by strategically stacking prepreg layers (plies) at defined orientations and locations within the laminate. Desired thicknesses and performance attributes are obtained by varying the number of plies and their angular placement within the lay-up.

When a laminate consists of a single ply or multiple plies aligned in the same direction, it is referred to as a lamina. In contrast, when plies are arranged at varying fiber orientations, typically ranging from –90° to +90°, the structure is termed a laminate [5]. The stacking sequence of a laminate is conventionally represented using bracket notation, such as [a/90/b/c/0/d/…], where each symbol denotes the fiber orientation of an individual ply. For example, the notation [45/0/–15/90/45] indicates a five-ply laminate with specific ply orientations [6].

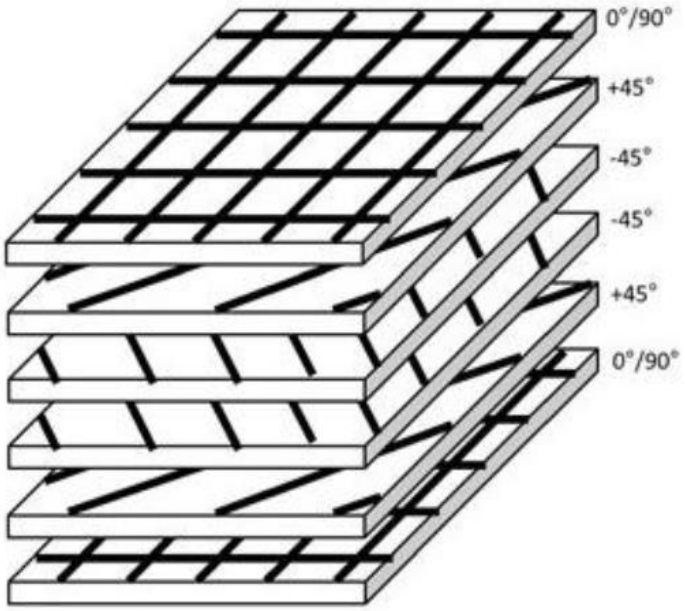

Figure 2.4: *Stacking of prepreg plies to a laminate with different angles of fibers*

Figure 2.4 illustrates the sequential stacking of prepreg plies at different fiber angles to form a multi-directional laminate [7]. The orientation and sequence of fiber layers play a critical role in

determining the laminate's overall mechanical behavior, including its stiffness distribution**,** damage tolerance**,** and failure mechanisms under various loading conditions.

2.1.4 Failure and Damage Mechanisms for Composite Laminates

When a structure becomes incapable of performing its intended function, it is defined as a failure. In engineering applications, failure does not always indicate total fracture; it can also refer to the material or system no longer meeting its design criteria. Several indicators are used to determine the failure mechanism, including stiffness degradation, yielding, fatigue life reduction, impact resistance loss, bending instability, and corrosion sensitivity.

In composite laminates, failure mechanisms are particularly important because these materials often exhibit localized damage modes before experiencing total structural failure. These localized forms of damage can significantly affect the laminate’s load-bearing capacity and overall performance, even if the structure appears intact. Therefore, in composite structures, the term "damage" is frequently used to describe preliminary forms of failure that precede full rupture.

Common damage mechanisms observed in composite laminates include:

- Splitting
- Buckling
- Fatigue
- Impact damage
- Creep and stress relaxation
- Delamination

Splitting occurs when fibers are oriented in a single direction and matrix adhesion is weak in the transverse direction. Under such conditions, longitudinal cracks may form parallel to the fiber direction. This damage is often triggered by in plane bending or localized stress concentrations, such as in bolted or pinned joints where wedge-like effects are present.

Buckling is a type of instability that can develop even under relatively low compressive loads and results in significant out-of-plane deformation. In composite laminates, buckling often initiates

delamination between plies. It can be mitigated by increasing structural stiffness, reducing unsupported lengths, or using thicker laminate sections.

Fatigue damage in composites differs from that in metals. While fatigue in steel typically involves crack initiation and growth due to cyclic loading until catastrophic failure occurs, fatigue in composite materials evolves through matrix cracking, fiber-matrix debonding, fiber breakage, and delamination. The accumulation of such damage is influenced by factors like fiber orientation, laminate sequence, loading conditions, and environmental exposure.

In composite laminates, fatigue damage does not typically occur through a single dominant crack, as in metals. Instead, multiple fatigue cracks may initiate simultaneously in different directions. Over time, these microcracks can grow, merge, and result in more extensive damage zones, potentially leading to delamination and a significant reduction in structural integrity [8].

Impact damage in composite laminates is often difficult to detect visually, especially from the impacted surface. This is due to the elastic nature of composite materials, which can absorb and distribute impact energy without immediately showing surface damage. However, internal damage such as matrix cracking, fiber breakage, and delamination may still occur beneath the surface, compromising the mechanical performance of the laminate.

Creep and stress relaxation are time-dependent deformation mechanisms observed in composite materials, particularly under long-term loading and elevated temperatures. In composite laminates, the fibers primarily carry the applied load, while the polymer matrix, often epoxy, helps transfer stress between fibers. Over time, stress redistribution from the matrix to the fibers can lead to creep. This phenomenon is especially sensitive to high temperatures and environmental conditions such as humidity or chemical exposure [9].

Delamination refers to the separation of adjacent plies within a composite laminate. It is considered one of the most critical failure modes, as it significantly reduces the load-carrying capacity, stiffness, and damage tolerance of the composite structure. Delamination may be initiated by out-of-plane stresses, impact events, or manufacturing defects, and once initiated, it can propagate under service loads, leading to further degradation of the laminate.

2.2 Production Methods

2.2.1 Electrospinning

Electrospinning has emerged as one of the most versatile and widely utilized techniques for the fabrication of nanofibers, owing to its relative simplicity, cost-effectiveness, and capability to produce continuous, non-woven fibrous mats with exceptionally high surface area to volume ratios. The large specific surface area of electrospun nanofibers renders them highly suitable for a broad range of advanced applications, including but not limited to tissue engineering, catalysis, biosensing, automotive components, defense technologies, and biomedical devices.

This technique enables the production of uniform, continuous nanofibers with controllable morphology and dimensions, which typically range from several hundred nanometers down to a few micrometers in diameter. A wide variety of polymers both natural and synthetic can be employed in the electrospinning process, making it a highly adaptable method for tailoring nanofiber properties to specific application requirements.

A conventional electrospinning system generally comprises three primary components: (i) a syringe pump equipped with interchangeable needle types (e.g., single, coaxial, or dual-capillary configurations), (ii) a high-voltage power supply capable of generating strong electrostatic fields, and (iii) a conductive collector that may take various geometries (e.g., planar, patterned, grooved, or rotating) to influence fiber alignment and deposition. A schematic representation of a typical electrospinning setup is provided in Figure 2.5.

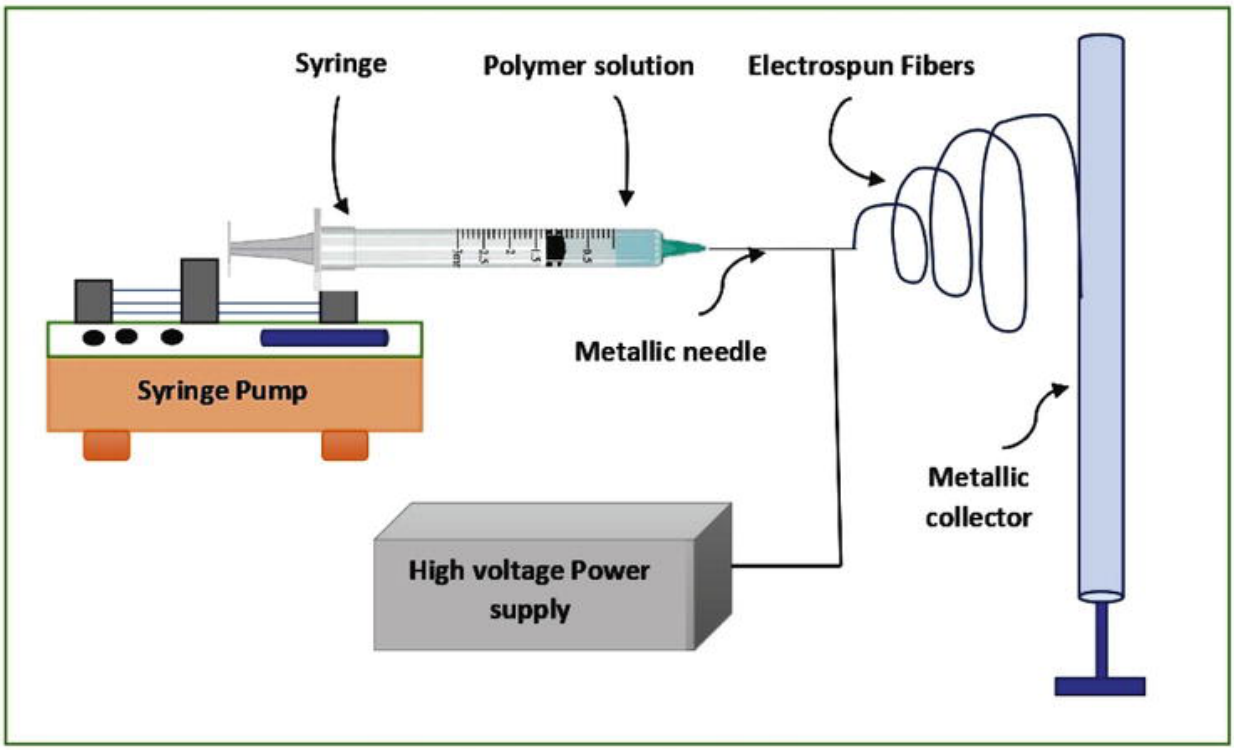

Figure 2.5: Schema about the electrospinning method

During the electrospinning process, environmental conditions such as temperature and relative humidity must be carefully controlled, as they significantly influence fiber morphology and uniformity. For this purpose, air conditioning systems are commonly employed to maintain stable ambient conditions throughout the process.

A high-voltage direct current (DC) power supply, typically in the range of several tens of kilovolts, is applied between the metallic collector and the syringe tip, which is usually fitted with a conductive needle. Under the influence of the strong electrostatic field generated, the polymer solution at the needle tip is subjected to electrostatic forces that overcome its surface tension. This results in the formation of a conical meniscus known as a Taylor Cone**.** Once the electrostatic force surpasses the cohesive forces within the droplet, a charged polymer jet is ejected from the apex of the cone toward the grounded collector.

As the polymer jet travels through the air, the solvent rapidly evaporates, leading to the solidification of the jet into ultrafine fibers. These fibers, still carrying residual charge, are

ultimately deposited onto the conductive collector surface, forming a non-woven mat of electrospun nanofibers.

2.2.1.1 Parameters of Electrospinning

The electrospinning process is influenced by a variety of parameters, which are commonly categorized into three main groups, as illustrated in Figure 2.6:

- Ambient condition parameters
- Polymer solution parameters
- Process condition parameters

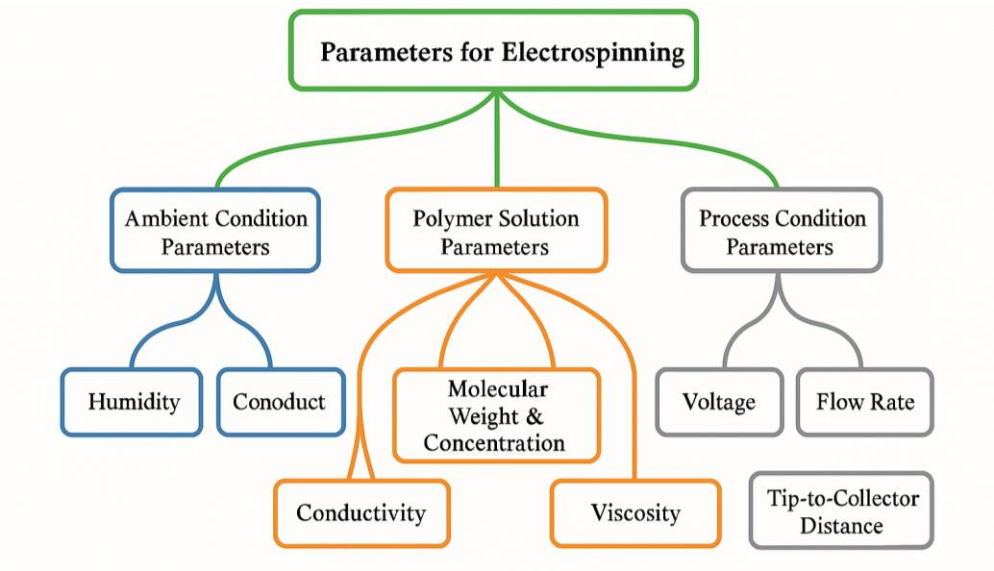

Figure 2.6: *Parameters of Electrospinning method*

Electrospinning is a highly sensitive process influenced by a variety of parameters that can significantly affect the morphology, diameter, and uniformity of the resulting nanofibers. These parameters are generally grouped into three categories: ambient conditions, polymer solution properties, and processing parameters. Key influential factors within each category are discussed below.

Ambient Condition Parameters

Humidity: Kim et al. [10] (2004) demonstrated that increasing relative humidity in the electrospinning environment leads to an increase in fiber diameter. High humidity slows the solvent evaporation rate, resulting in incomplete solvent removal when the jet reaches the collector.

Residual solvent within the fiber promotes pore formation on the fiber surface upon complete drying, thus affecting surface morphology.

Temperature: Temperature impacts both the viscosity of the polymer solution and the solvent evaporation rate. Elevated temperatures reduce solution viscosity and accelerate solvent evaporation, facilitating the formation of finer fibers. Consequently, an increase in ambient temperature generally correlates with a decrease in fiber diameter [11].

Polymer Solution Parameters

Dielectric Constant: An increase in the dielectric constant of the solution enhances its ability to store electrostatic charges. This results in a greater elongation of the polymer jet, yielding fibers with reduced diameters. Lee et al. [12] showed that poly(ε-caprolactone) (PCL), while insoluble in N, -dimethylformamide (DMF), can be dissolved in methylene chloride (MC). However, DMF has a higher dielectric constant than MC. Therefore, blending DMF with MC increases the dielectric properties of the solution, producing finer nanofibers.

Electrical Conductivity: Electrospinning relies on the repulsion of like charges within the jet to stretch and thin the polymer stream. Increasing the conductivity of the polymer solution enhances charge density in the jet, promoting elongation and reducing bead formation. In cases where intrinsic conductivity is insufficient, salts may be added to the solution to increase charge density and facilitate the production of smoother, finer fibers [13].

Molecular Weight and Concentration: Low molecular weight polymers tend to produce beaded structures due to insufficient chain entanglement, which is crucial for jet stability [14]. Furthermore, polymer molecular weight influences solution concentration and viscosity. Ki et al. [15] observed that higher polymer concentrations lead to increased fiber diameters due to the increased viscosity and entanglement density of the solution.

Viscosity: Solution viscosity, primarily governed by polymer concentration and molecular weight, plays a critical role in fiber formation. Low-viscosity solutions tend to produce beads rather than fibers, a phenomenon known as electrospraying. Conversely, excessively high viscosity can cause the solution to dry at the needle tip, hindering continuous fiber formation. Thus, optimizing solution viscosity is essential for producing uniform, bead-free nanofibers.

Surface Tension: For successful electrospinning, the surface tension of the polymer solution must be overcome by the applied electrostatic forces. High surface tension can inhibit jet formation and lead to bead defects. Solvents with inherently lower surface tension can be used to reduce the overall surface tension of the spinning solution, improving fiber quality.

Process Condition Parameters

Applied Voltage: There is a direct relationship between applied voltage and the electrostatic forces acting on the polymer jet. Megelski et al. [16] reported that increasing the applied voltage results in enhanced jet stretching, leading to a decrease in fiber diameter, provided other parameters remain constant.

Flow Rate: The flow rate of the polymer solution affects the volume of material ejected towards the collector. Higher flow rates result in larger bead formation and increased fiber diameters due to insufficient stretching time and slower solvent evaporation. Optimal flow rates must be maintained to balance fiber uniformity and production efficiency.

Tip-to-Collector Distance (TCD): TCD influences both the electric field strength and the flight time of the polymer jet. Shorter distances increase electric field intensity but reduce the time available for solvent evaporation, leading to wet fibers and irregular morphologies. Conversely, increasing TCD allows more time for jet elongation and solvent evaporation, producing finer and more uniform fibers [17].

2.2.2 Heat Press Method

During the curing process of composite materials, the heat press method (also known as hot pressing) is a widely utilized technique that involves the simultaneous application of controlled heat and mechanical pressure. This method plays a critical role in enhancing the quality and performance of thermosetting and thermoplastic composite laminates by improving their structural integrity and surface finish.

One of the primary advantages of the heat press method is its ability to significantly reduce the presence of voids and trapped air within the laminate structure. By applying uniform pressure

across the laminate surface, the method facilitates intimate contact between layers, ensuring that the resin fully wets the fibers and fills interlaminar spaces. This leads to a denser and more homogenous material, which in turn enhances the mechanical properties such as tensile strength, interlaminar shear strength, and impact resistance.

Moreover, the elevated temperature provided during the heat press cycle accelerates the cross-linking reaction in thermosetting resins (epoxy), enabling a faster and more uniform curing process. In thermoplastic-based composites, heat assists in softening the matrix, allowing for better fusion between layers and improved crystallinity, which directly influences stiffness and thermal stability.

Another critical function of the heat press technique is the maintenance of fiber orientation and the suppression of fiber wrinkling or shifting during curing. Proper consolidation of fiber layers under pressure ensures optimal stress transfer between fibers and matrix, leading to superior load-bearing performance. In addition, the heat press process provides precise control over the fiber to resin volume ratio**,** which is a key factor in determining the final mechanical behavior of the composite part. Excess resin can be expelled under pressure, preventing resin-rich zones that may act as weak points.

From a manufacturing perspective, the heat press method allows for reproducibility and scalability, making it suitable for both laboratory-scale research and medium-volume industrial production. It is commonly used in the fabrication of flat or moderately contoured composite parts in industries such as automotive, consumer electronics, and sporting goods. Compared to methods like vacuum bagging, the heat press technique can offer higher consolidation pressures and shorter cycle times, albeit with limitations on part geometry and size.

The heat press method is an effective and efficient technique for the fabrication of high-performance composite laminates. Its ability to combine heat and pressure in a controlled environment not only improves the physical and mechanical characteristics of the final product but also ensures manufacturing consistency attributes that are critical in applications demanding structural reliability and material precision.

Figure 2.7: *HURSAN heat press machine*

2.3 Polycaprolactone (PCL)

PCL is a thermoplastic, biodegradable polyester with good thermal processability, low melting point, and low viscosity. It is synthesized through the polymerization of ε-caprolactone. Due to its weak barrier properties and poor mechanical performance, attributed to its low melting point, the application of PCL as a biodegradable polymer in the packaging industry is limited. To expand its range of applications, PCL is often blended with other polymers (such as cellulose propionate, polylactic acid, and cellulose acetate butyrate) to improve stress crack resistance, dyeability, and adhesion (Navarro-Baena et al., 2016). The chemical structure of PCL is presented in Figure 2.8.

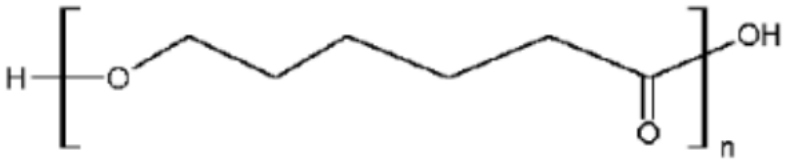

Figure 2.8: *The chemical structure of PCL (Mahapatro and Singh, 2011).*

Polycaprolactone (PCL) is a semi-crystalline polymer due to its regular structure, with a melting point ranging from 59°C to 64°C and a low glass transition temperature at -60°C (Pillai and Sharma, 2010). Its physical properties are presented in Table 2.3. This polymer exhibits both rigidity and flexibility (Mergaert et al., 1994), and displays a rubber-like behavior at body temperature due to its high permeability.

PCL is soluble at room temperature in a wide range of solvents such as dichloromethane, chloroform, tetrahydrofuran, benzene, carbon tetrachloride, toluene, and cyclohexanone. However, it exhibits poor solubility in acetone, dimethylformamide, ethyl acetate, and acetonitrile, and is insoluble in ethers and alcohols (Coulembier et al., 2006).

The physical, chemical, and mechanical properties of PCL can be effectively modified through copolymerization and blending (Azimi et al., 2014). Blending has been shown to alter the physical and mechanical properties along with the biodegradation behavior. For instance, blending PCL with polylactide (PLA) decreases its Young's modulus and tensile strength, while PCL/cellulose composites can enhance crystallinity and crystallization temperature. Blending PCL with proteins reduces water sensitivity compared to protein-based plastics alone and improves stability under ambient conditions. Additionally, copolymerization can lead to changes in chemical characteristics that indirectly affect properties such as solubility, crystallinity, and degradation behavior (Dash and Konkimalla, 2012).

Table 2.3: *The physical properties of PCL (Labet and Thielemans, 2009).*

Properties	Ranges
Average molecular weight (Mn; $g \cdot mol^{-1}$)	530,000 – 630,000
Density (ρ; $g \cdot cm^{-3}$)	1.071 – 1.200
Glass transition temperature (Tg; °C)	(-65) – (-60)
Melting point (Tm; °C)	59 – 64
Decomposition temperature (°C)	350
Inherent viscosity (η_{inh}; $cm^3 \cdot g^{-1}$)	100 – 130
Intrinsic viscosity (η; $cm^3 \cdot g^{-1}$)	0.9
Tensile strength (σ; MPa)	4 – 785
Young's modulus (E; GPa)	0.21 – 1.44

2.4 Curing Process

The curing process refers to the irreversible transformation of a polymer resin system, typically thermosetting in nature, into a solid, crosslinked structure through a chemical reaction. In composite materials, particularly those involving thermosetting matrices like epoxy, curing plays a central role in defining the final mechanical, thermal, and chemical performance of the material. This transformation is initiated and sustained through external stimuli, most commonly heat, but also through chemical initiators or ultraviolet radiation, depending on the system.

Curing involves the crosslinking of reactive functional groups within the polymer matrix, such as the reaction of epoxide rings with amine or anhydride hardeners in epoxy systems. As these covalent bonds form, the polymer chains are interconnected into a three-dimensional network, converting the material from a viscous or gel-like state into a rigid and insoluble thermoset. This crosslinking significantly enhances properties such as modulus, dimensional stability, heat resistance, and environmental durability.

The chemical kinetics of curing are governed by several factors, including the nature and ratio of the resin and hardener, temperature, time, and the presence of catalysts or additives. Curing kinetics can typically be described by autocatalytic or diffusion-controlled models, and are often

investigated using thermal analysis methods. The degree of cure, which quantifies the extent of crosslinking, is a critical measure and is directly related to the composite's mechanical integrity and thermal behavior.

Environmental conditions such as ambient humidity and oxygen content can influence curing efficiency and may result in phenomena like surface inhibition or uneven crosslinking. Similarly, the physical dimensions and thermal conductivity of the curing system can lead to gradients in cure level, potentially introducing residual stresses or microstructural defects.

In composite manufacturing, especially in high-performance fiber-reinforced systems, the curing process must be carefully optimized to ensure uniform matrix distribution and adequate adhesion to the reinforcing phase. Improper curing may lead to voids, incomplete polymerization, or interfacial debonding, all of which degrade composite reliability.

Ultimately, the curing process not only solidifies the resin but also establishes the internal architecture and long-term performance characteristics of the composite material. Its control is essential in both laboratory-scale research and industrial-scale production.

2.5 Tensile Test

Tensile tests are conducted for material selection, quality assurance, and predicting behavior under different loading conditions. They help compare materials during development and ensure compliance with specifications.

Strength is a key factor, measured by the stress needed for plastic deformation or the maximum stress a material can withstand. These values, used with safety factors, guide engineering design. Ductility, indicating how much a material can deform before fracturing, is crucial for ensuring toughness. Low ductility often means low resistance to fracture under other loads. Elastic properties are also important but require special techniques like ultrasonic methods for accurate measurement.

Consider the typical tensile specimen shown in Figure 2.9. Tensile specimens are designed with enlarged ends or shoulders for gripping, while the most critical part is the gage section, which has a reduced cross-sectional area to localize deformation and failure. The gage length, centered

in the reduced section, must be sufficiently large to avoid constraints from the ends. If the gage length is too short relative to its diameter, the stress distribution becomes complex.

Different gripping methods ensure that the specimen is securely held during testing. These methods include threaded grips, pinned ends, butt ends, and wedge grips, among others. The primary goal of gripping is to prevent slippage or failure at the grip section while minimizing bending forces.

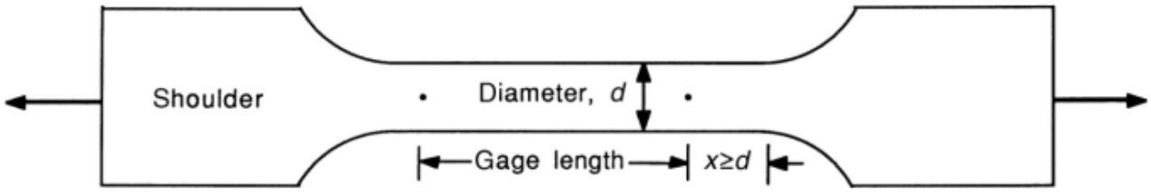

Figure 2.9: *Tensile Specimen measurements*

2.5.1 Stress and Strain

Objects naturally deform under tensile or compressive loads, though this deformation is often too small to see. It can be calculated using key parameters, primarily the applied force and cross-sectional area.

Greater force results in greater deformation, but this force does not act uniformly throughout the body. The cross-sectional area also plays a role deformation is directly proportional to force and inversely proportional to area. This relationship defines stress (Pa) as force per unit area.

Since cross-sectional area varies in a body, deformation is not uniform. Larger areas increase intermolecular forces, resisting external forces, whereas smaller areas reduce this resistance.

A tensile test involves mounting the specimen in a machine, such as those described in the previous section, and subjecting it to tension. The tensile force is recorded as a function of the increase in gage length.

2.6 Charpy Impact Test

The notched-bar impact test is a standard method used to assess the behavior of materials subjected to sudden, high-speed loading conditions, particularly when stress concentrations are introduced by a notch. This test provides critical insight into how a material fractures under dynamic loading and is particularly useful in distinguishing between brittle and ductile failure modes.

In brittle materials, where plastic deformation is minimal or absent, the area under the stress-strain curve is relatively small. As a result, these materials absorb only a limited amount of energy before fracturing, which corresponds to low toughness.

The fracture surfaces resulting from impact testing further illustrate these differences in material behavior. Brittle fractures typically exhibit smooth, shiny surfaces with well-defined crystalline patterns, indicating a rapid crack propagation with little plastic deformation. In contrast, ductile fractures show more complex, rough surfaces with significant distortion, often referred to as fibrous fracture surfaces. These features are indicative of plastic flow before rupture and are generally aligned at approximately a 45° angle to the direction of the applied tensile stress this angle corresponds to the direction of maximum shear stress.

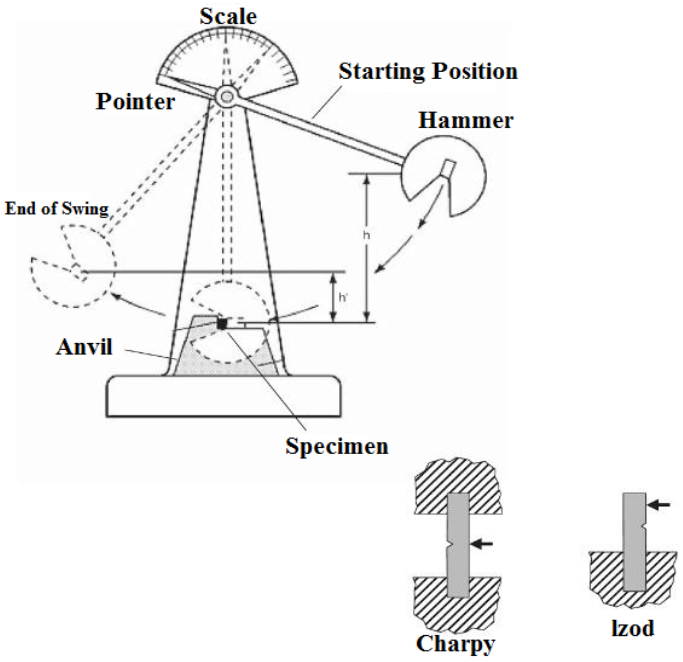

Figure 2.12: *Apparatus for impact testing of materials*

The DBTT (ductile-brittle transition temperature) is a critical parameter in the design and application of structural materials, as it defines the lowest temperature at which the material can be safely used without the risk of brittle fracture. Below this transition temperature, the material may fail catastrophically under impact or dynamic loading, even if it would behave ductility at higher temperatures.

The standard Charpy impact test primarily measures the total energy absorbed by a specimen during fracture, providing a general indication of its toughness. However, when more detailed information about the fracture process is needed, an instrumented Charpy impact test can be employed.

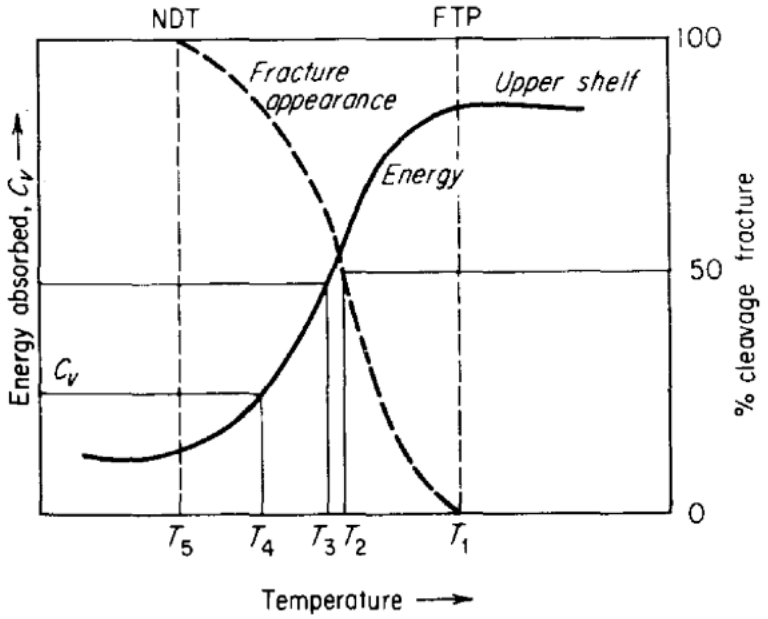

Figure 2.13: *Various criteria of transition temperature obtained from Charpy tests*

An idealized load-time curve from an instrumented Charpy test is shown schematically in Figure-4. This curve captures the variation of applied load with respect to time from the moment of impact until complete fracture. With this data, the fracture process can be broken down into two distinct energy components:

Fracture initiation energy: the energy required to initiate a crack at the notch.

Fracture propagation energy: the energy consumed in propagating the crack through the remainder of the specimen.

3. Materials and Methods

In this section, the concepts to be used in this project are explained through references taken from similar research papers on composite materials published.

3.1. Materials

In this study, UN3082 is the epoxy resin, UN2259 is the hardener.

***Table 3.1**: Physical properties of Epoxy*

Epoxy Resin UN3082	
Density [g/cm³]	1.11-1.14
Viscosity [mPa·s]	600 - 800
Refractory index	1.571 - 1.578

***Table 3.2**: Physical properties of hardener*

Curing Agent UN2259	
Density [g/cm³]	0.982 – 0.990
Viscosity [mPa·s]	20 - 30
Refractory index	1.484 - 1.494

Measuring conditions: measured at 25°. (Momentive Specialty Chemicals) 300g/m^2 unidirectional carbon fiber fabric was used.

***Table 3.3**: Physical properties of Carbon Fiber Fabric*

Carbon Fiber	
Resin Consumption	346 g / m^2
Laminate Thickness	0.48 mm
Laminate Weight	646 g / m^2

3.2 Optimization of Ply Orientation

In order to obtain optimal performance in the tensile and impact tests to be conducted, it is essential to design the stacking sequence of the composite laminates with the most appropriate ply orientations. To achieve this:

- The plies must be arranged symmetrically with respect to the laminate's mid-plane. This symmetry ensures balanced mechanical behavior and minimizes warping or twisting under load.
- To provide high in-plane stiffness and maximize the elastic modulus in both the longitudinal (x) and transverse (y) directions, it is necessary to include plies oriented at 0°, ±45°, and 90° angles.
- Additionally, to avoid localized weaknesses and stress concentrations, plies with identical fiber orientations should not be positioned directly adjacent to one another.

With these design considerations in mind, various laminate configurations featuring different ply orientations were modeled and evaluated using MATLAB. The numerical analysis was carried out based on the Tsai-Wu failure criterion, under the application of a uniaxial tensile load of **1** kN in the y-direction which corresponds to the direction aligned with the fibers in the 0° plies. The MATLAB code used for this analysis is provided in the Appendix [15].

Types	**Orientations**
A	[+0° / 45° / -45° / 90° / 90° / -45° / 45° / 0°]
B	[+45° / −45° / 0° / 90°/ 90° / 0° / −45° / +45°]
C	[0° / +45° / 90° / −45° /−45° / 90° / 45° / 0°]
D	[−45° / 90° / +45° / 0° / 0° / +45° / 90° / −45°]
E	[90° / +45° / 0° / −45° /−45° / 0° / +45° / 90°]
F	[−45° / 0° / +45° / 90° / 90° / +45° / 0° / −45°]
G	[−45° / 90° / 0° / +45°/ +45° / 0° / 90° / −45°]
H	[−45° / 0° / +45° / 90°/ 90° / +45° / 0° / −45°]
I	[+45° / 90° / −45° / 0° / 0° / −45° / 90° / +45°]
J	[0° / 90° / −45° / +45° / +45°/ −45° / 90° / 0°]

Since the strength ratios of the tested samples remained consistent, no additional iterations are required. Based on both the strength ratios and the ease of manufacturing, laminate A was determined to be the most appropriate choice for production. (The Tsai-Wu failure criterion was applied to every ply in each laminate, and the ply with the highest SR value was used for evaluation.)

The following formulas and concepts were used to determine the suitable orientation. The same formulas are also used for theoretical estimations of tensile strength in later sections.

The extension stiffness matrix is defined by the following formula:

$$A_{ij} = \sum_{k=1}^{n} \left[\bar{Q}_{ij}\right]_k (h_k - h_{k-1}) \quad (1)$$

The coupling stiffness matrix is defined by the following formula:

$$B_{ij} = \frac{1}{2} \sum_{k=1}^{n} \left[\bar{Q}_{ij}\right]_k ({h_k}^2 - {h_{k-1}}^2) \quad (2)$$

The coupling stiffness matrix represents the relationship between **in-plane force** to **in-plane strain** in the x-y-z-direction.

The following formula defines the bending stiffness matrix:

$$D_{ij} = \frac{1}{3} \sum_{k=1}^{n} \left[\bar{Q}_{ij}\right]_k ({h_k}^3 - {h_{k-1}}^3) \quad (3)$$

The midplane strains and curvatures can be found by solving the following matrix:

$$\begin{bmatrix} N_x \\ N_y \\ N_{xy} \\ M_x \\ M_y \\ M_{xy} \end{bmatrix} = \begin{bmatrix} A & B \\ B & D \end{bmatrix} \begin{bmatrix} {\varepsilon^0}_x \\ {\varepsilon^0}_y \\ {\gamma^0}_{xy} \\ {\kappa^0}_x \\ {\kappa^0}_y \\ {\kappa^0}_{xy} \end{bmatrix}$$

The ABBD matrix combines extensional stiffness matrix (A), coupling stiffness matrix (B), and bending stiffness matric (D), through which midplane strains ($\varepsilon^0{}_x$, $\varepsilon^0{}_y$, $\varepsilon^0{}_{xy}$) and midplane curvatures ($\kappa^0{}_x$, $\kappa^0{}_y$, $\kappa^0{}_{xy}$) is calculated.

The Global Strain for a laminate can be calculated as:

$$\begin{bmatrix} \varepsilon_x \\ \varepsilon_y \\ \gamma_{xy} \end{bmatrix} = \begin{bmatrix} \varepsilon^0{}_x \\ \varepsilon^0{}_y \\ \gamma^0{}_{xy} \end{bmatrix} + z \begin{bmatrix} \kappa_x \\ \kappa_y \\ \kappa_{xy} \end{bmatrix}$$

Since the laminate is symmetric in nature, the curvature of the laminate is zero in value, making the Global strain values equal to the laminate extension.

Local Stress for A^o ply can be calculated using Transformation Matrix [T], where $\sin(A)$ and $\cos(A)$, are used

$$[\,T\,] = \begin{bmatrix} c^2 & s^2 & 2sc \\ s^2 & c^2 & -2sc \\ -sc & sc & c^2 - s^2 \end{bmatrix}$$

For symmetric laminates, when coupling stiffness matrix [B] = 0, it can be shown that $[A^*] = [A]^{-1}$ and $[D^*] = [D]^{-1}$.

Through $[A^*]$, also known as the **Extensional Compliance Matrix**, calculating Effective In-Plane Engineering Constants is possible.

$[D^*]$, also known as the **Bending Compliance Matrix** through which calculating Effective Flexural Engineering Constants is possible.

Tsai – Wu Failure Criteria can be tested by the following equation:

$$H_1\sigma_1 + H_2\sigma_2 + H_6\tau_{12} + H_{11}\,\sigma_1^2 + H_{22}\,\sigma_2^2 + H_{66}\,\tau_{12}^2 + 2H_{12}\sigma_1\sigma_2 < 1 \qquad (4)$$

When the equation in left hand side is defined as SI, then the lamina follows the following conditions.

- $SI < 1; ply\ is\ safe$

- $SI \geq 1;\ failure\ occurs, as\ inequality\ is\ violated.$

3.3 Production Methods

3.3.1 Electrospinning Process

In this study, nanofiber mats were fabricated using the electrospinning technique with poly(ε-caprolactone) (PCL) as the polymer base. Electrospinning is a well-established method for producing nanoscale fibers by applying a high-voltage electric field to a polymer solution, resulting in continuous fiber formation with a high surface area-to-volume ratio.

***Figure 3.1**: A photo from the Single Nozzle Electrospinning machine*

To prepare the electrospinning solution, 4 grams of PCL were dissolved in 16 grams of Dimethylformamide (DMF), yielding a total solution mass of 20 grams. The mixture was stirred

at 400 rpm and maintained at 70 °C until a completely homogeneous solution was obtained. These conditions ensured proper dissolution of PCL and stable solution viscosity for spinning

Figure 3.2: *A photo about amount of PCL And DMF*

The prepared polymer solution was then loaded into a syringe connected to a stainless-steel needle. The electrospinning process was conducted under the following optimized parameters:

- **Applied voltage**: 25 kV
- **Flow rate**: 2 mL/hr
- **Collector rotation speed**: 500 rpm

In this part of the study, flow rates of 0.5 mL, 1 mL, and 1.5 mL were tested. However, fluctuations were observed in PCL production at these flow rates, indicating a lack of homogeneity. Additionally, stirring speeds of 300 rpm and 400 rpm were also tested, but similarly, no homogeneity was achieved.

***Figure 3.3**: Photo from the electrospun process*

Under these conditions, seven nanofiber mats were successfully produced and collected on a rotating drum wrapped with aluminum foil. The resulting PCL nanofibers exhibited uniform morphology and good web formation, suitable for potential use as reinforcing interlayers or surface modification layers in composite laminates.

3.3.2 Preparation of Specimens

In this experiment, composite plates were manufactured using carbon fiber fabric and an epoxy matrix without any nanoparticle additives. Four sets of specimens were produced for mechanical testing. All samples were composed of 8 layers of unidirectional carbon fiber, arranged according to a pre-defined stacking sequence to achieve desired mechanical characteristics.

Before lay-up, carbon fiber fabrics were cut to specific dimensions corresponding to their orientations (0°, 90°, ±45°). Firstly, the carbon fiber fabric was cut to appropriate sizes as shown in Figure-2.3. The 250x300 mm^2 fabric in the image is for 0- and 90-degree plies, while the 250x300 mm^2 fabric is for 45-degree plies. The epoxy resin and hardener were prepared in a 5:1 weight ratio, thoroughly mixed to initiate the curing reaction. No nanoparticles were added to the epoxy mixture.

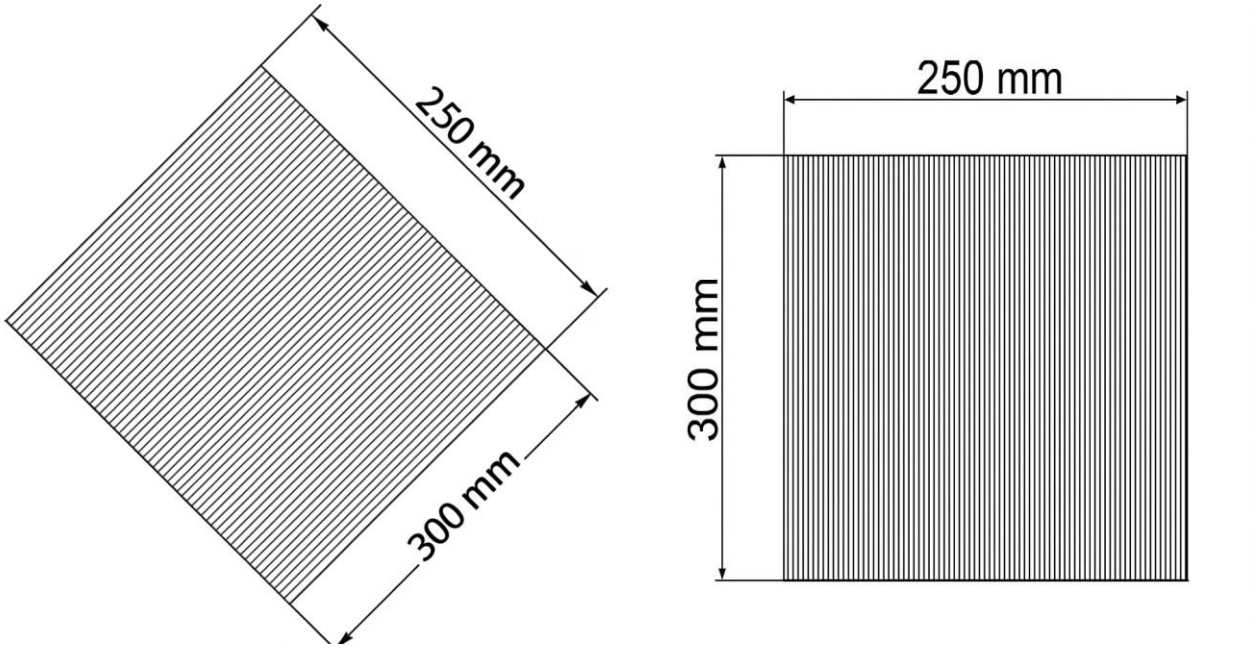

Figure 3.4: *Carbon fiber (left side) and PCL (right side) fabric measurements*

Figure 3.5: *Applying epoxy-hardener mixture*

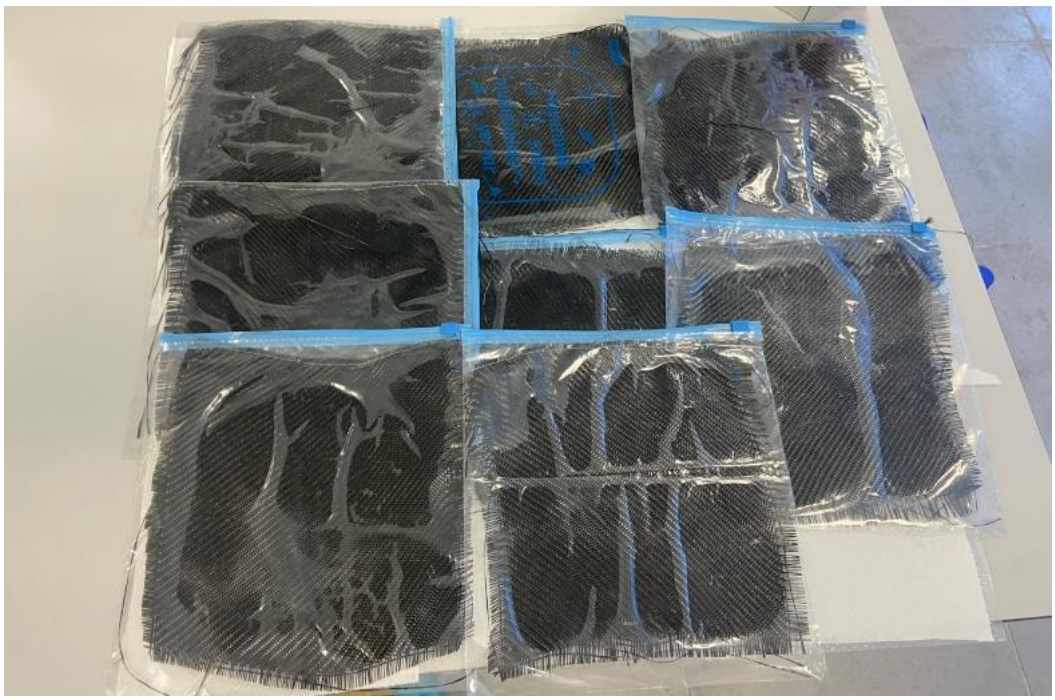

Figure 3.6*: Carbon fibers in vacuum bags*

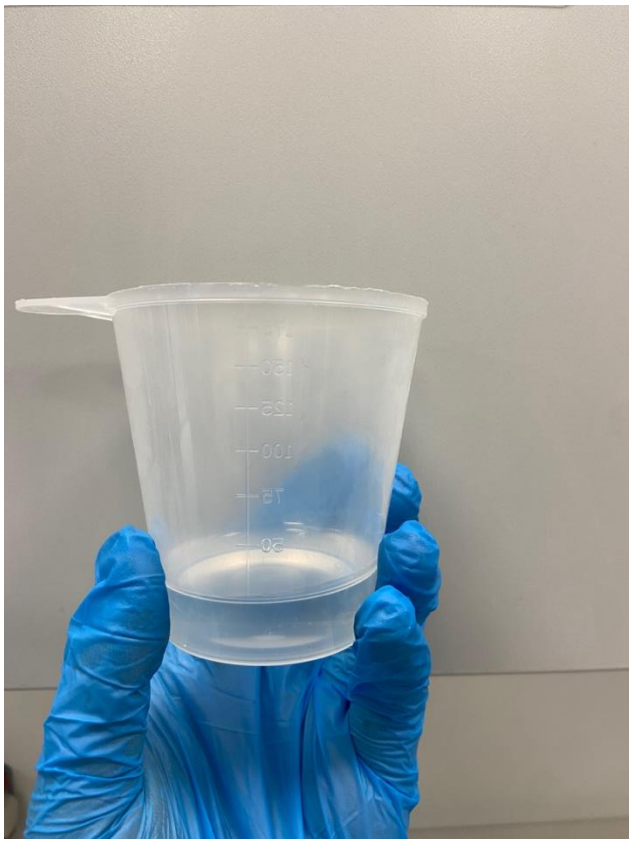

Figure 3.7: *Epoxy and hardener mixture*

During lay-up, epoxy was applied manually to each fabric layer individually, using a brush. This ensured that each ply was properly impregnated before the next layer was added. After, all 7 plies were stacked and saturated with resin, the laminate was placed between two flat metal plates with release films to prevent sticking. The assembled lay-up was then transferred to a hot press machine, where it was cured under heat and pressure in two stages:

- **First stage**: 60 °C for 15 minutes (pre-curing phase),
- **Second stage**: 120 °C for 90 minutes (full curing phase).

Constant pressure was applied during both stages to ensure proper consolidation of the laminate and minimize void formation. After pressing, the cured composite plates were removed from the mold and allowed to cool at room temperature. The final plates were then trimmed and cut into standardized test specimens according to relevant ASTM standards.

3.3.3 Hot Pressing Technique

In this study, the composite specimens were produced using the hot press molding method. This technique involves applying heat and pressure simultaneously to cure the laminate structure, which allows for better control over the consolidation and thickness of the final product. Compared to vacuum bagging, hot pressing can offer a more uniform distribution of resin and eliminate voids more effectively in a shorter period.

***Figure 3.8**: PCL nanofiber with carbon epoxy layering*

***Figure 3.9**: The heat press process*

During production, multiple carbon fiber fabric layers were stacked in a predefined orientation. No nanoparticles were added to the matrix in this study. A two-part epoxy resin system was used, with epoxy and hardener mixed at a 5:1 weight ratio, ensuring proper chemical curing. The mixed epoxy was manually applied between each fabric layer one by one, using a brush to ensure complete wetting and uniform distribution.

After stacking and impregnating the layers, the layup was placed between two metal plates lined with non-stick release film. The setup was then positioned inside a hot press machine, where a defined amount of pressure and temperature were applied. The curing process took place under these controlled conditions to form a consolidated and uniform composite plate.

Once cured, the composite plates were removed from the press, cooled to room temperature, and then cut into standardized specimen shapes for mechanical testing

***Figure 3.10**: Heat press process and values from the process*

3.4 Testing Methods:

The final plates were trimmed in various samples for tensile testing and Charpy impact testing as shown below. Among them, the 2 best specimens were selected for tensile testing and the 2 best specimens were selected for Charpy impact testing.

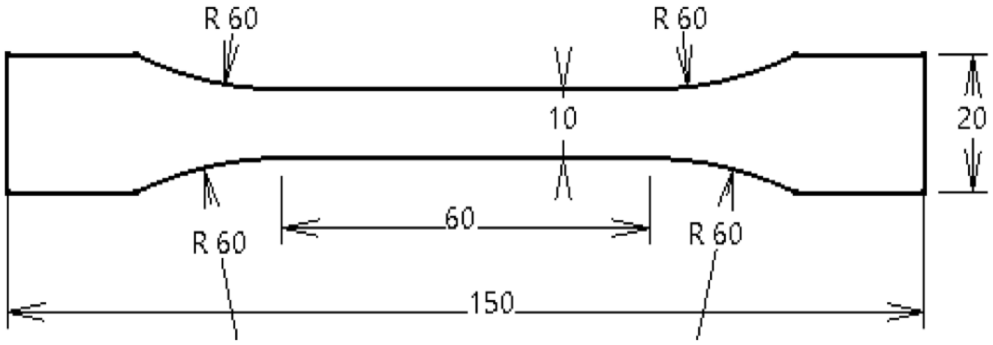

***Figure 3.11:** Dimensions of the tensile test specimen. The units are in mm*

***Figure 3.12**: Different samples obtained from hot pressed plate*

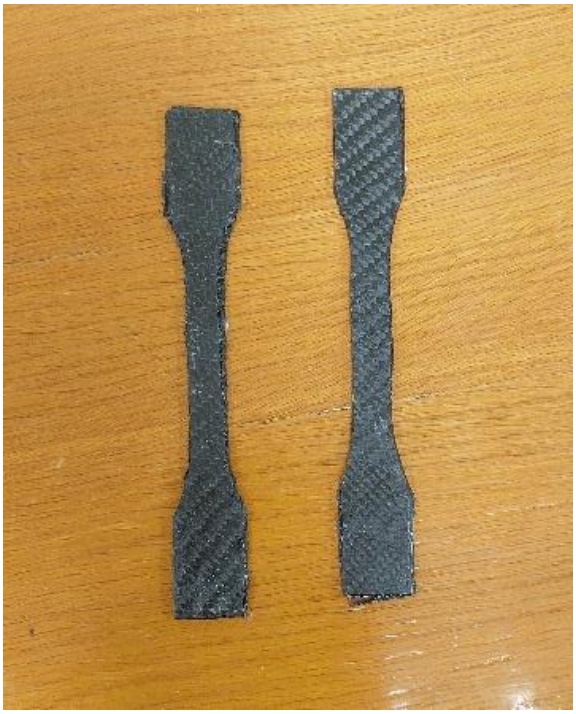

***Figure 3.13:** Tensile testing Specimen used (Sample 1 and Sample 2)*

Figure 3.14: *Sample setup for tensile testing*

Both the test samples for tensile testing had thickness value ranging around 2.30 mm. The tensile test was conducted with the help of SHIMADZU AGS – X series testing machine. The samples were tested for its mechanical characteristics through the stress – strain curve produced by the TRAPEZIUM X software. The testing gauge cross speed for the machine was 5 mm/min and the method in which the samples were secured is demonstrated in the figure below.

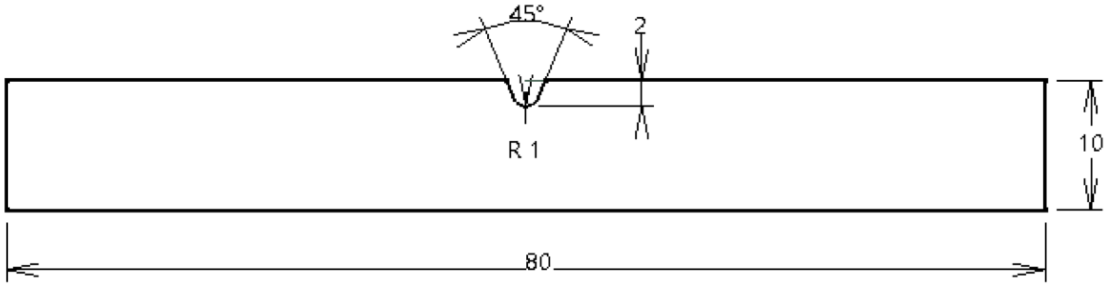

Figure 3.15: *Dimensions of the Charpy impact test specimen. The units are in mm.*

Figure 3.16: *Charpy Impact Test Specimen used (Sample 1 and Sample 2)*

Engineering stress, or nominal stress, σ is defined as:

$$\sigma = \frac{F}{A} \ (in\ Pa) \tag{5}$$

Where;

F: Force Acting on the Area (N)

A: Cross-Sectional Area (m^2)

σ: Stress (Pa)

Engineering strain, or nominal strain, is defined as:

$$\varepsilon = \frac{L'}{L_0} = \frac{L_0 - L}{L_0} \tag{6}$$

Where;

L_0: The Original Length (m)

L: The Deformed Length (m)

L': Change in Length (m)

ε: Strain

The specimens were tested in a Charpy Impact Tester, INSTRON CEAST 9050 model, which assists in measuring the impact resistance and toughness of the Electrospun PCL carbon epoxy

composite. It does it with the help of a large, centrally mounted pendulum arm, which is released to strike the specimen. The energy absorbed by the specimen during fracture is then inspected with the help of graphs produced.

Both samples had a thickness of around 2.50 mm, with a 45-degree v – V-shaped dent on one side of the sample, and an impact velocity of 3.80 m/s was applied. A 50 J pendulum was used.

Young's modulus (E). The relationship among stress (σ), strain (ε), and Young's modulus is expressed as:

$$\sigma = E \times \varepsilon \tag{7}$$

True stress and strain are calculated as:

$$\sigma_T = \sigma\left(\frac{L}{L_0}\right) \tag{8}$$

$$\varepsilon_T = \ln\left(\frac{L}{L_0}\right) \tag{9}$$

Where;

σ_T: True Stress

ε_T: True Strain

Figure 3.17: *Charpy Impact Tester – INSTRON CEAST 9050*

The modulus of resilience is calculated using the following formula:

$$U_R = \frac{\sigma_Y^2}{2\ x\ E} \tag{10}$$

Where:

U_R: the modulus of resilience (J/m^3),

σ_Y: the yield strength (Pa),

E: the modulus of elasticity (Pa).

Both modulus of toughness and modulus of resilience are essential for proper material selection and design in engineering. Understanding the balance between these properties helps engineers ensure that materials can withstand not only static loads but also dynamic or impact forces, providing safety and long-term durability.

4. RESULTS & DISCUSSION

4.1. Tensile Test:

The two sample specimens were tested using a tensile testing machine, and with the help of TRAPZIUM software, the force and stroke applied to the sample were converted into a stress–strain curve, which provides critical data on the behavior and mechanical properties of the samples under increasing load. The Figure below compares the stress–strain behavior of two specimens, with the red line representing the Sample 1 specimen and the black line representing the Sample 2 specimen.

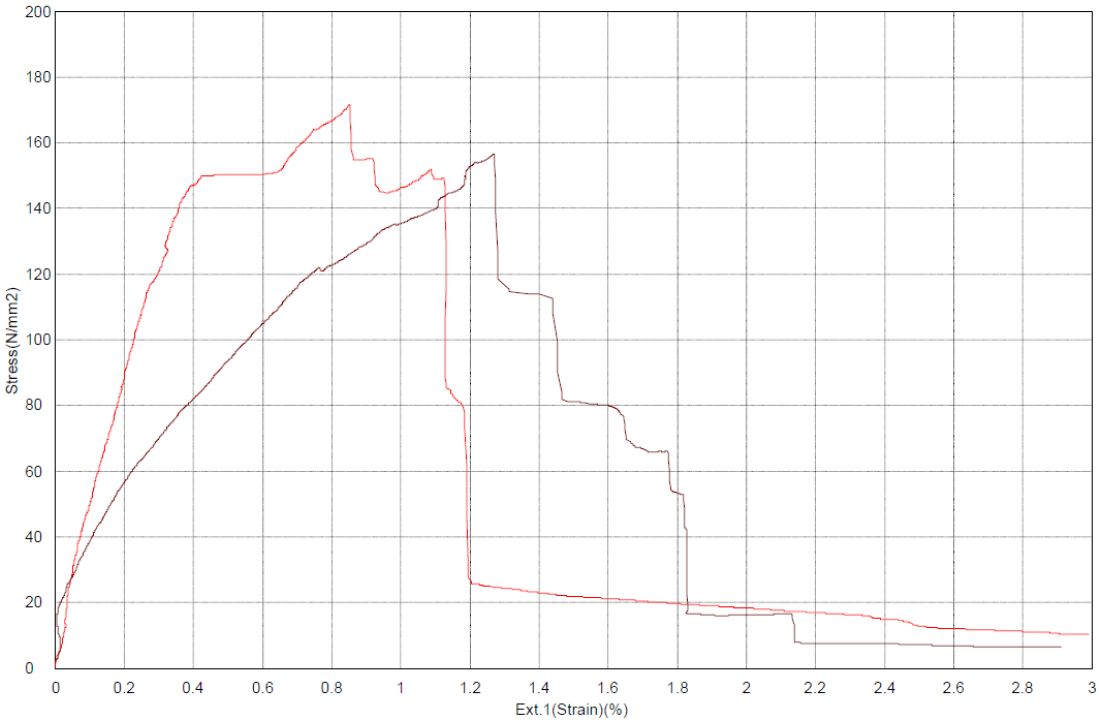

Figure 4.1: *Stress – Strain graph of Sample 1(red) and Sample 2(black)*

Both samples demonstrate anisotropic mechanical behavior of advanced laminated composites. These materials show linear elastic behavior up to a point of failure and have no yield point as they follow a brittle failure mechanism. This behavior can be attributed to the thermoset epoxy matrix. They are crosslinked polymers that have high stiffness and strength but lack ductility, which aids in their overall brittleness. Also, given the samples are carbon fiber dominated, which are known for high strength, high stiffness reinforcement with brittle fracture mode, the global tensile behavior remains predominantly linear and brittle in nature as observed

in the tensile testing. From the graph, we have obtained the following properties for both the samples:

Table 4.1: *Observed Mechanical Properties for Sample 1 (Red line)*

Ultimate Tensile Strength (MPa)	Failure Strain (%)	Elastic Modulus (GPa)
171.7	1.20	120

Table 4.2: *Observed Mechanical Properties for Sample 2 (Blue line)*

Ultimate Tensile Strength (MPa)	Failure Strain (%)	Elastic Modulus (GPa)
156.7	1.41 – 1.60	105

For sample 1, the curve is linear with slight curvature and reaches its Ultimate Tensile Strength of 171.7 MPa at around 0.82 % strain, and after 1.18 % strain, there is a first sudden drop. There was a crackling sound observed during this time, while testing, and when inspected, it was found that one layer of the carbon fiber had broken apart, even though the other 6 plies remained intact with a cracking noise. This explains the drop in stress value. At 1.20 % strain, the sample reaches failure strain, as indicated by the flat curve. This behavior is typical of fiber-dominated composite failure, where delamination/ ply failure precedes total failure.

Figure 4.2: *Delamination seen in Sample 1 after tensile testing*

For sample 2, the curve has less slope and reaches its Ultimate Tensile Strength of 156.7 MPa at 1.22 % strain, which occurs later in sample 2, when compared with sample 1. Gradual decrease starts right after, at around 1.30 % strain, and reaches final failure at around 1.4 % - 1.6% strain. Small load fluctuations are also seen during this period. These might be because sample 2 does not face any delamination during the entire stress, hence it has a gradual decrease rather than a sudden one.

Localized excess epoxy distribution could introduce stress concentration, which might have weakened sample 2. under tensile loading. The difference in the concentration of distribution of PCL nanofibers might have also affected the load transfer between fiber and matrix, hence contributing to different UTS values. However, the difference between the UTS values is under 10%, hence making both sample behaviors consistent with each other.

Despite having lower strength, sample 2 exhibited a noticeably higher failure strain, which is indicative of enhanced toughness, likely caused due to a slight difference in microstructural uniformity of fiber and matrix in the sample. These also allow failure to occur across a longer strain gradually, rather than immediately, as seen in Sample 1, which occurred due to delamination.

Given the lower UTS value, sample 2 has a 12.5 % less steeper curve, hence a lower value of elastic modulus, which indicates less effective load transfer in sample 2.

Trapped air during the hot press process can also have contributed to decreasing both UTS and Failure strain values. The epoxy applied across the carbon fiber might not have been evenly distributed, which aided in causing localized stress concentration, resulting in a decrease in the failure strain values.

The loading rate of 5mm/min might have been too fast for detecting early damage initiation. The visible resin-rich zone in both samples might have disturbed the potential of the samples. High–modulus fiber (T700) might have been too brittle for the system, given the samples had little to no time before breakage.

Oxygen Plasma treatment can be done on carbon fibers to increase their surface energy, to improve epoxy wetting, and to reduce localized stress concentrations in the composite. Core-shell electrospinning with PCL as core and PAN as shell can be used together for the interleaving, as the PAN shell can bond to epoxy and increase the PCL energy absorbing capability. The matrix can be toughened by adding SIO_2 to increase modules while adding CTBN (carboxyl-terminated butadiene acrylonitrile) rubber to improve toughness. NBR (Nitrile Butadiene Rubber) can also be added with PCL to enhance the fracture toughness of carbon fiber composite [17]. Combining glass fiber with carbon fiber can also increase the impact resistance of the composite.

4.1.1 Theoretical Estimation for Tensile Testing:

Theoretical estimations are done using CLT (Classical Laminate Theory) predictions technique with the help of MATLAB to find the properties of carbon–fiber epoxy composites, without the addition of any electrospun PCL. A total of 8 plies were used in symmetry with angles [0^o, 45^o, -45^o,90^o, and -90^o]. The code computes the theoretical value under a uniaxial tensile load of 1kN (aligned with 0^o ply). The average value of the properties is used in the calculation.

Table 4.3: *Mechanical Properties of Carbon/Epoxy Composites.*

Mechanical Properties	Units
Longitudinal elastic modulus	70-75 (GPa)
Transverse elastic modulus	5.5-6.5 (GPa)
Poisson's ratios	0.28
Shear modulus	5-6 (GPa)
Ultimate longitudinal tensile strength	600-750 (MPa)
Ultimate longitudinal compressive strength	20-30 (MPa)
Ultimate transverse tensile strength	100-150 (MPa)
Ultimate in-plane shear strength	30-40 (MPa)

For 8 plies, the best stacking sequence with all 5 angles is: [0^o / 45^o / -45^o / 90^o / 90^o / -45^o/ 45^o/ 0^o] as 0^o plies improve load bearing, 45^o balances shear, and 90^o includes transverse stability.

Table 4.4: *Global Stresses (Pa)*

Ply Angle	σ_x	σ_y	T_{xy}
0^o	-2.10×10^3	1.95×10^5	0.00
45^o	1.53×10^4	8.54×10^4	4.07×10^4
-45^o	15.3×10^4	8.54×10^4	-4.07×10^4
90^o	-5.80×10^3	1.32×10^4	0.00

Table 4.5: *Local Stresses (Pa)*

Ply Angle	σ_x	σ_y	T_{xy}
0º	-2.10×10^{3}	1.95×10^{5}	0.00
45º	1.53×10^{4}	8.54×10^{4}	4.07×10^{4}
-45º	15.3×10^{4}	8.54×10^{4}	-4.07×10^{4}
90º	-5.80×10^{3}	1.32×10^{4}	0.00

Table 4.6: *Global strains*

Ply Angle	ε_x	ε_y	γ_{xy}
0º	-3.00×10^{-4}	2.00×10^{-3}	0.00
45º	-1.20×10^{-3}	2.50×10^{-3}	1.80×10^{-3}
-45º	-1.20×10^{-3}	2.50×10^{-3}	-1.80×10^{-3}
90º	-1.10×10^{-3}	2.20×10^{-3}	0.00

Table 4.7: *Local strains*

Ply Angle	ε_x	ε_y	γ_{xy}
0º	2.00×10^{-3}	3.00×10^{-4}	0.00
45º	1.10×10^{-3}	1.10×10^{-3}	2.50×10^{-3}
-45º	1.10×10^{-3}	1.10×10^{-3}	-2.50×10^{-3}
90º	-1.10×10^{-3}	-1.10×10^{-3}	0.00

Studying the global and local stresses, the highest stress occurs on 0º plies with $\sigma_y = \sigma_1 = 195.6$ MPa with Tsai–Wu FI value of 0.29, which is the safest and most stable plate. The 45-degree plies are critical in shear, as only they have T_{xy} values with Tsai-Wu FI value being the highest among the angles with FI = 0.73.

When comparing it with experimental data, which were (156.7 MPa and 171.7 MPa) for 2 samples respectively, they have + 14-25% deviation when compared with the theoretical value of

195.6 MPa. Under CLT assumptions, the composite is under perfect bonding, no defects with linear elasticity, and does not consider delamination, resin-rich zones, or localized stress concentrations. That's why the predicted UTS under CLT is slightly higher than the actual value obtained.

PCL nanofibers are known to reduce UTS slightly by promoting non-catastrophic failure while adding toughness to the material. So, despite adding PCL nanofibers, the UTS value is still less than the maximum strength of the carbon-epoxy composite. For better estimation, progressive damage models can be used to capture and predict ply-to-ply failure. Fiber volume fraction can be measured and adjusted according to the requirement. Also, increasing 0^o plies can be added for higher UTS. The most reliable and useful way of improving the UTS is through the use of hybrid interleaves, using extra material like PAN, CNTs, or NBR alongside PCL during electrospinning.

Then, observing global and local strains, for all angles, ε_y in the loading direction has the highest value, showing that the fiber direction dominates in the composite. The 45-degree plies measure shear strain critical for failure, whereas the 90-degree ply measures the transverse strain, which measures matrix-sensitive.

Experimental Failure Strain lies in the range of 1.20 % - 1.60 % due to non-linear effects as seen in stress-strain curve during tensile testing and when compared with the CLT prediction which gives an estimation of 0.20 – 0.25 % with linear assumption, it can be observed that adding PCL electrospun nanofiber has increased the toughness of the composite significantly, including slight ductility and increasing strain capacity of the composite.

Adding PCL prevents the immediate failure of the composite under loading/impact, which generally occurs in carbon/epoxy composites. They also form a slight ductile interlayer and reduce stress concentration at ply boundaries.

4.2. Charpy Impact Test:

The impact test was done using a 50 J pendulum hammer as impact energy, 3.80 m/s of impact velocity, with the hammer starting at around 150 degrees. Both of the samples eventually broke under impact; however, sample 1 went through the impact test three times before cracking,

whereas sample 2 only had to go through one impact before cracking.

For specimens, the force (N) versus time (ms) can be used to calculate the electrospun PCL carbon-fiber epoxy composite's ability to resist crack propagation. Also, the graph also indicates how much energy the material can absorb before breaking. The peak of the curve displays the maximum force that the materials can absorb.

Sample 1 went through three impacts before cracking. The graphs obtained for sample 1 are displayed below with yellow, black, and green curves.

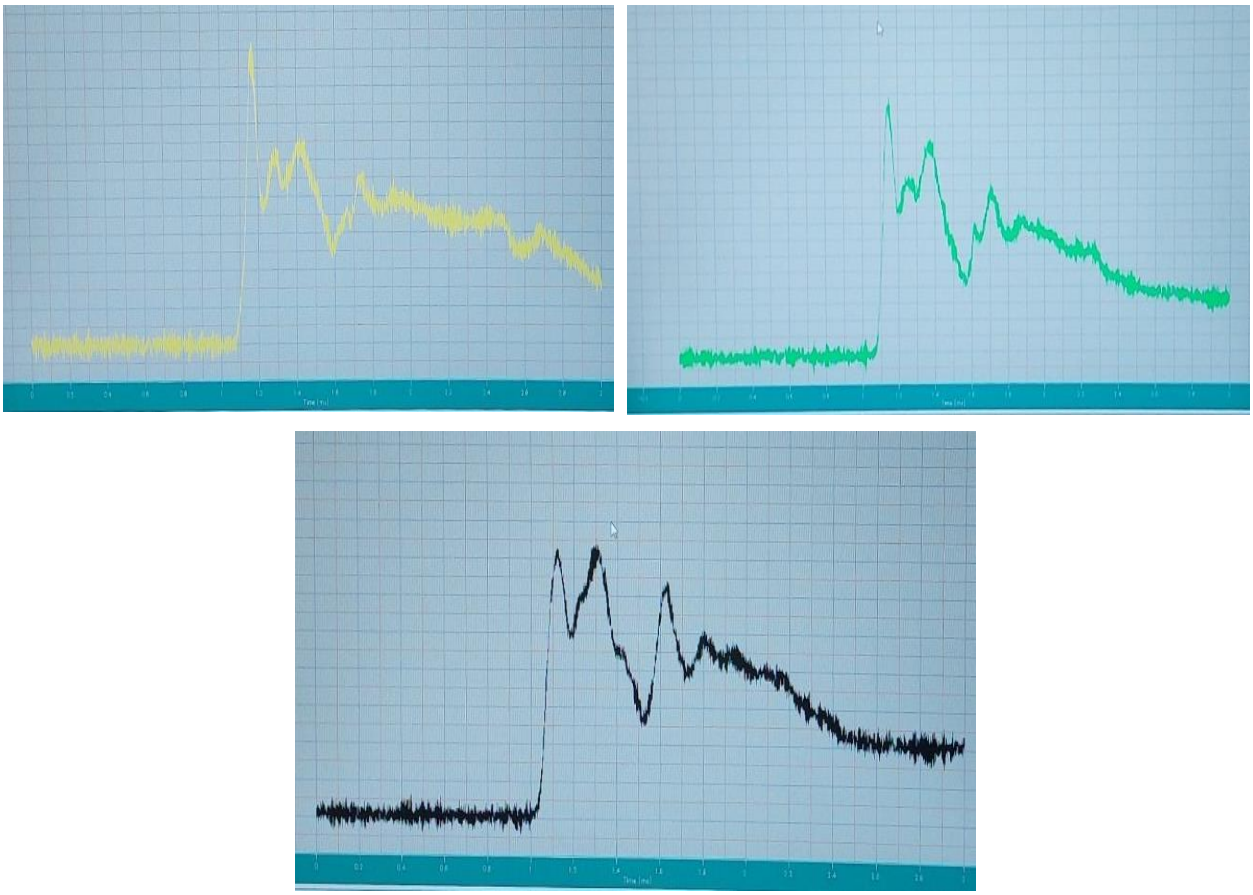

Figure 4.3: *Force versus time graph for Sample 1 (yellow, green, and black curves)*

Each curve shows multiple small peaks and a more gradual energy dissipation, as the sample did not fail after the first impact. The gradual reduction instead of sudden failure indicates progressive internal damage with each test. The force drops and rebounds might represent

microcracking, matrix deformation, fiber pull-out, or delamination. This behavior points to more ductility, better energy absorption, or a layer internal damage mechanism.

Sample 2 immediately reached the breaking point after the first impact test. The red curve is used to represent the force and time graph.

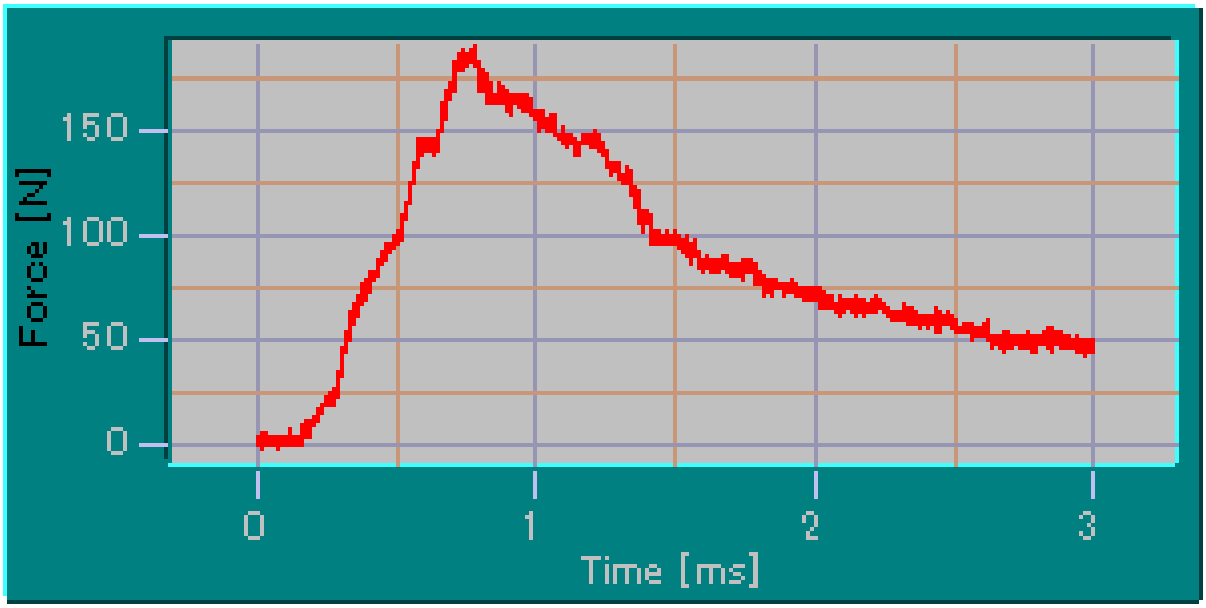

Figure 4.4: *Force versus time graph for Sample 2 (red curve)*

The single peak reaches the maximum force, followed by a steady drop. This indicates that sample 2 absorbed a high amount of energy, which indicates a high strength value, and then gradually fractured completely. The curve also indicates very low toughness, as energy is absorbed in a quick period.

Samples 1 and 2, after impact testing, are shown below:

Figure 4.5: *Sample 1, after Charpy Impact Test*

Figure 4.6: *Sample 2, after Charpy Impact Test*

Both samples went through different failure modes as shown. Sample 1 has better energy dissipation, with debonding and fiber sliding absorbing energy over time. They may have lower initial strength but much higher toughness and resistance to gradual failure. Whereas Sample 2 has very high initial strength absorption, but lower toughness than Sample 1. However, given the brittle characteristics of the composite, it is more useful for the material to absorb as much

strength/energy as possible before breakage.

Sample 2, given their behavior, has a very high fiber volume fraction but maybe poor wetting of epoxy. However, the brittle epoxy matrix behavior is dominating as expected. But the quick breakage may be due to insufficient electrospun fiber entanglement or non-uniform dispersion. It can also be due to localized stress concentration caused by non-uniform wetting of epoxy.

5. FEASIBILITY & COST ANALYSIS

To determine the production cost of a composite product, several critical cost components must be evaluated, including material expenses, capital equipment, and labor. The following breakdown presents the primary cost drivers for the composite manufacturing process:

Raw Materials: The composite production utilized various essential materials such as carbon plies, resin, hardener, vacuum sealing tape, vacuum bag, PCL, DMF, and breather cloth. These materials contribute significantly to the total cost, with carbon plies and resin being the most expensive items. Prices vary depending on quantity used and market conditions. For instance, 1 m^2 of carbon plies costs ৳843.88, while 100 g of resin costs ৳850.

Capital Costs: Some components and equipment, like the pump and infusion vacuum hose, are categorized as capital costs. While the pump cost was not specified, 1 meter of infusion vacuum hose added ৳26.05 to the total. These tools are generally reusable but must still be considered for initial investment.

Labor and Processing Costs: The project included 7 labor units, amounting to ৳350. Labor costs reflect the cutting, finishing, and handling of materials throughout the process. These tasks are often semi-automated or manual, requiring skilled operation to ensure proper composite fabrication.

Overhead and Utility Considerations: Though not itemized in this specific analysis, factors such as electricity usage, equipment maintenance, and workspace requirements also contribute to overall manufacturing costs and should be considered in broader financial planning.

Table 5.1: *Cost analysis of the project.*

		Manufacturing Costs	Number or Amount	Cost
Manufacturing Costs	**Material Cost**	Carbon Plies	$1m^2$	৳ 843.88
		Resin	100 g	৳ 850
		Hardener	25 g	৳ 350
		Vacuum Sealing Tape	15 m	৳ 346.73
		Vacuum Bag	$1\ m^2$	৳ 250
		PCL	16 g	৳ 16
		DMF	112 mL	৳ 120
		Breather Cloth	$1.5m^2$	৳ 58.70
	Capital Cost	Pump	1	-
		Infusion Vacuum Hose	1 m	৳ 26.05
Industry Costs	**Cutting and Finishing Cost**	Labor Cost	7	৳ 350
			TOTAL	৳ 3.211,36

The total production cost of the composite project was calculated as **৳3,211.36**, encompassing both materials and labor.

6. CONCLUSION AND FUTURE WORKS

This project investigated the enhancement of the mechanical properties of thermosetting carbon/fiber epoxy laminates through the incorporation of electrospun Polycaprolactone (PCL) nanofiber interlayers. The project focused on fabricating composite laminates using electrospinning and hot press techniques and evaluating their mechanical properties through Tensile testing and Charpy Impact Tests.

A total of 8 plies of carbon fiber planes with symmetric orientation, including angles of 0 °, 45 °, and 90 °, were used alongside 7 layers of electrospun PCL, layered between the carbon fiber planes. The observations done on this project provided valuable insights into the effectiveness of PCL nanofibers in improving the mechanical characteristics of composite materials.

During tensile testing of 2 identical samples, sample 1 exhibited an ultimate tensile strength (UTS) of 171.7 MPa with a failure strain of 1.20 %. The stress–strain curve demonstrated a linear response up to the point of initial ply failure, which was followed by a sudden stress drop, which was likely caused by delamination and localized fiber breakage of the sample during testing Whereas, sample 2 exhibited a lesser UTS value of 156.7 MPa, with a higher failure strain ranging from 1.41 % to 1.60 %, suggesting a more enhanced ductility and toughness when compared to sample 1.

Both samples displayed significantly higher failure strain%, way above the Classical Laminate Theory (CLT) theoretical estimates of 0.2 – 0.5 % for any carbon/fiber epoxy composites. This suggests that the inclusion of Electrospun PCL nanofibers significantly improved the toughness of the laminates. However, CLT prediction for UTS of the composites was around 195.6 MPa, almost 14-25 % higher than the obtained experimental UTS values. This trade–off is common due to the inclusion of PCL nanofibers, as they enhance the energy dissipation and delay failure in the composite while slightly reducing their load transfer efficiency.

The delamination experienced by sample 1 ply failure can be attributed to weak interlaminar bonding. This weakness significantly reduces the laminate's ability to redistribute stress, leading to sudden failure. So, improving fiber–matrix adhesion is essential to delaying the delamination

process. One approach involves using oxygen plasma treatment to improve the surface of carbon fiber used, which in turn increases its surface energy, which then aids in improving wetting and chemical bonding with the epoxy matrix. Authors in [18] used oxygen plasma treatment of carbon fibers, which led to a 25 % increase in overall interlaminar shear strength due to more enhanced fiber-matrix interaction.

Another way can be the use of hybrid interleaves, which has gained quite the attention as a strategy to toughen the interlaminar region. The authors in [19] incorporated Polyacrylonitrile (PAN) nanofibers and reinforcing PCL interlayers with Carbon Nanotubes (CNTs) which significantly improves the Mode 1 interlaminar fracture toughness of carbon/epoxy laminates by more than 80%. Similarly, the authors in [20] demonstrated that integration of CNT reinforced PCL interlayer resulted in simultaneous improvements in toughness and UTS by creating a multi-scale reinforcement network.

During the Charpy impact tests for 2 identical samples, the difference in failure behavior between them reveals various insights into the effectiveness of the interlaminar toughening mechanism of the composite. Sample 1 successfully withstood three consecutive impacts before cracking, indicating a progressive damage accumulation and high energy dissipation capacity. The force-time curve exhibited multiple peaks, suggesting delamination of the composite, which was visibly confirmed after testing for sample 1. This response reflects a toughened interlaminar region, where PCL likely assisted in stress redistribution and delayed failure. Whereas sample 2 failed after a single impact, displaying a sharp and singular peak in the force-time graph, displaying a brittle fracture characteristic with minimal energy absorption. The failure may be attributed to void formation or non-uniform distribution of PCL nanofibers.

Throughout both tests, a common problem of resin-rich zones had significantly reduced the overall potential of the samples. Resin-rich zones are localized regions within composite laminates where the epoxy matrix accumulates excessively, due to uneven resin flow. These zones often produce localized stress concentrations and aid in reducing interlaminar shear strength, void formation, and premature failure under mechanical loading.

Authors of [21] used the Vacuum-Assisted Resin Infusion (VARI) technique, which improves resin distribution and minimizes voids by using a vacuum to draw resin uniformly through dry fiber preforms. VARI technique significantly reduced resin-rich zones, improved fiber wetting, and enhanced interlaminar properties compared to hand lay-up techniques.

Overall, the electrospun PCL nanofibers significantly improved the composite's ability to absorb energy and resist crack propagation, addressing the inherent brittleness of carbon-fiber/epoxy matrices. The PCL nanofibers also promoted gradual failure modes, instead of immediate brittle fracture, which is critical for structural applications. The electrospinning also allows precise control over fiber morphology and distribution, allowing for customized changes to the mechanical properties of the composite.

The electrospun PCL nanofiber enhanced carbon fiber epoxy composite, tested in this project, is ideal in applications where toughness of the material holds priority over its pure strength, like in bicycle frames, hockey sticks, tennis rackets, etc. It can also be used where progressive failure is required and energy absorption is the key, like helmets and panels. PCL is also hydrophobic, so they have certain resistance to water absorption, making it useful in boat hulls and submarine panels.

And if its delamination resistance is improved by using Hybrid interleaves like PCL + PAN, PCL + CNTs and PCL+ NBR, the composite can prove very useful in applications like aircraft wings skins, helicopter rotor blades, where preventing catastrophic delamination under cyclic loads is more essential while maintaining its structural integration and providing its lightweight properties.

REFERENCES

[1] Essential Chemical Industry. (2013). *Composites*. Retrieved August 25, 2018, from http://www.essentialchemicalindustry.org/materials-and-applications/composites.html

[2] Staab, G. (2015). *Laminar Composites* (2nd ed.). Elsevier Ltd.

[3] Nijssen, R. P. L. (2015). *Composite Materials: An Introduction*. Taniguchi, N., Nishiwaki, T., & Kawada, H. (2007). Tensile strength of unidirectional CFRP laminate under high strain rate. *Advanced Composites Materials, Official Journal of the Japan Society for Composite Materials*, 16(2), 167–180.

[4] Thomas, G. P. (2013). Composite Prepregs – Manufacturing, Benefits and Applications. Retrieved from https://www.azom.com/article.aspx?ArticleID=8353

[5] Campbell, F. C. (2010). *Introduction to Composite Materials* (p. 630)

[6] Reddy, J. N., & Miravete, A. (1995). *Practical Analysis of Composite Laminates*. CRC Press.

[7] Kim, G. T., et al. (2004). Effect of humidity on the microstructures of electrospun polystyrene nanofibers. *Microsc. Soc. Am.*, 554–555.

[8] Mit-uppatham, C., Nithitanakul, M., & Supaphol, P. (2004). Ultrafine electrospun polyamide-6 fibers: Effect of solution conditions on morphology and average fiber diameter. *Macromolecular Chemistry and Physics*, 6, 2327–2338.

[9] Lee, K. H., Kim, H. Y., Khil, M. S., Ra, Y. M., & Lee, D. R. (2003). Characterization of nano-structured poly(ε-caprolactone) nonwoven mats via electrospinning. *Polymer*, 44, 1287–1294.

[10] Almetwally, A. A., El-Sakhawy, M., Elshakankery, M. H., & Kasem, M. H. (2017). Technology of nano-fibers: Production techniques and properties – Critical review. *Journal of Textile Association*, 78(1), 5–14.

[11] McKee, M. G., Wilkes, G. L., Colby, R. H., & Long, T. E. (2004). Correlations of solution rheology with electrospun fiber formation of linear and branched polyesters. *Macromolecules*, 37, 1760–1767.

[12] Ki, C. S., Baek, D. H., Gang, K. D., Lee, K. H., Um, I. C., & Park, Y. H. (2005). Characterization of gelatin nanofiber prepared from gelatin-formic acid solution. *Polymer (Guildf).*, 46, 5094–5102.

[13] Megelski, S., Stephens, J. S., Chase, D. B., & Rabolt, J. F. (2002). Micro- and nanostructured surface morphology on electrospun polymer fibers. *Macromolecules*, 35, 8456–8466.

[14] Zhang, F., Zhang, Z., Liu, Y., Cheng, W., Huang, Y., & Leng, J. (2015). Thermosetting epoxy reinforced shape memory composite microfiber membranes: Fabrication, structure and properties. *Composites Part A: Applied Science and Manufacturing*, 76, 54–61. https://doi.org/10.1016/j.compositesa.2015.05.004

[15] Song, X., Gao, J., Zheng, N., Zhou, H., & Mai, Y. W. (2021). Interlaminar toughening in carbon fiber/epoxy composites interleaved with CNT decorated polycaprolactone nanofibers. *Composites Communications*, 24, 100622. https://doi.org/10.1016/j.coco.2020.100622

[16] Jang, H. S., Oh, J. H., & Lee, D. H. (2021). Intrinsic brittleness of epoxy matrix and delamination susceptibility: Efficient improvement in fracture toughness of laminated composites using functionalized polyacrylonitrile nanofibers. *Polymers*, 13(15), 2544. https://www.ncbi.nlm.nih.gov/pmc/articles/PMC8347688/

[17] Umer, R., & Sultan, M. T. H. (2022). Development of electrospun hybrid nanofibers as interleaves: Improving interlaminar fracture toughness and compression after impact strength of carbon fiber/epoxy composites using polyethersulfone nanofibers. *Polymer Composites*, 43(4), 2132–2145. https://doi.org/10.1002/pc.29336

[18] Yao, Y., Zhang, H., Zhang, Z., & Wang, B. (2007). Novel carbon fiber/epoxy composite toughened by electrospun polysulfone nanofibers. *Journal of Applied Polymer Science*, 104(1), 120–126. https://www.researchgate.net/publication/248268694

[19] Bhattacharya, M., & Jana, S. (2022). PEO nanofibers as epoxy toughener for effective CFRP delamination hindrance. *ACS Omega*, 7(18), 15793–15803. https://doi.org/10.1021/acsomega.2c01189

[20] Kang, H., Zhang, C., Liu, T., & Leng, J. (2021). Electrospun thermosetting carbon nanotube–epoxy nanofibers. *National Science Foundation Repository*. https://par.nsf.gov/servlets/purl/10319831

[21] Xie, T., & Mather, P. T. (2017). Epoxy/polycaprolactone systems with triple-shape memory effect. *Polymers*, 9(6), 256. https://www.ncbi.nlm.nih.gov/pmc/articles/PMC5452858/

[22] Irfan, M., Ahmad, Z., & Khan, M. (2024). A brief review on electrospun polymer derived carbon fibers for EMI shielding. *Functional Composite Materials*, 5(1). https://functionalcompositematerials.springeropen.com/articles/10.1186/s42252-024-00060-8

[23] Jang, H. S., Oh, J. H., & Lee, D. H. (2021). Mechanisms enhancing interlaminar fracture toughness: Functionalized polyacrylonitrile nanofibers in laminated composites. *Polymers*, 13(15), 2544. https://www.ncbi.nlm.nih.gov/pmc/articles/PMC8347688/

[24] Bhattacharya, M., & Jana, S. (2022). Ductility of PCL and energy dissipation: PEO nanofibers as epoxy toughener for CFRP. *ACS Omega*, 7(18), 15793–15803. https://doi.org/10.1021/acsomega.2c01189

[25] Umer, R., & Sultan, M. T. H. (2022). Combination of PEN's rigidity and PCL's flexibility: Interlaminar fracture toughness in CFRP. *Polymer Composites*, 43(4), 2132–2145. https://doi.org/10.1002/pc.29336

[26] Yao, Y., Zhang, H., Zhang, Z., & Wang, B. (2007). Thermal stability of PEN in epoxy composite toughening. *Journal of Applied Polymer Science*, 104(1), 120–126. https://www.researchgate.net/publication/248268694

[27] Xie, T., & Mather, P. T. (2017). Phase separation of PCL nanofibers during curing: Triple-shape memory effect. *Polymers*, 9(6), 256. https://www.ncbi.nlm.nih.gov/pmc/articles/PMC5452858/

[28] Jang, H. S., Oh, J. H., & Lee, D. H. (2021). Quantitative improvements in mechanical properties with functionalized PAN nanofibers. *Polymers*, 13(15), 2544. https://www.ncbi.nlm.nih.gov/pmc/articles/PMC8347688/

[29] Yan, C., Li, Y., & Zhou, X. (2020). Rubbery nanofibrous interleaves enhance fracture toughness and damping of CFRP laminates. *Materials & Design*, 194, 109049. https://doi.org/10.1016/j.matdes.2020.109049

[30] Yu, H., Yang, W., & Zhao, H. (2014). Effect of plasma treatment on interfacial properties of carbon fiber/epoxy composites. *Applied Surface Science*, 314, 1016–1023. https://doi.org/10.1016/j.apsusc.2014.04.103

[31] Zhang, D., & Ma, Y. (2012). Improvement of interlaminar fracture toughness of CFRP laminates using PAN-based nanofiber mats. *Composite Structures*, 94(4), 1554–1560. https://doi.org/10.1016/j.compstruct.2012.02.004

[32] Jin, F. L., & Park, S. J. (2018). Carbon nanotube-reinforced PCL nanofiber interleaves for enhancing toughness of laminated composites. *Composites Science and Technology*, 166, 65–73. https://doi.org/10.1016/j.compscitech.2018.03.024

APPENDIX

MATLAB code of optimization of ply orientations:

```
% Material properties (unidirectional carbon fiber/epoxy)
E1 = 72.5e3;   % MPa
E2 = 6e3;      % MPa
nu12 = 0.28;
G12 = 5.5e3;   % MPa
t_ply = 0.125; % mm (ply thickness)

% Strength properties (Tsai-Wu)
S1t = 675; S1c = 600; S2t = 25; S2c = 20; T12 = 35; % MPa

% Optimal stacking sequence (including ±90°)
angles = [0, 45, -45, 90, -45, 45, 0]; % [0/45/-45/90/-45/45/0]

% ABD matrix calculation
Q11 = E1 / (1 - nu12*(nu12*E2/E1));
Q22 = E2 / (1 - nu12*(nu12*E2/E1));
Q12 = nu12 * E2 / (1 - nu12*(nu12*E2/E1));
Q66 = G12;
Q = [Q11, Q12, 0; Q12, Q22, 0; 0, 0, Q66];

A = zeros(3); B = zeros(3); D = zeros(3);
for k = 1:length(angles)
    theta = angles(k);
    c = cosd(theta); s = sind(theta);
    T = [c^2, s^2, 2*c*s; s^2, c^2, -2*c*s; -c*s, c*s, c^2-s^2];
    Qbar = inv(T) * Q * inv(T)';
    z_k = -7*t_ply/2 + k*t_ply;
    z_k_minus_1 = z_k - t_ply;
    A = A + Qbar * (z_k - z_k_minus_1);
    B = B + 0.5 * Qbar * (z_k^2 - z_k_minus_1^2);
    D = D + (1/3) * Qbar * (z_k^3 - z_k_minus_1^3);
end

% Applied load (1 kN over 25.4 mm width)
N_y = 1000 / 25.4; % N/mm
N = [0; N_y; 0]; M = [0; 0; 0];
ABD = [A, B; B, D];
strains_curvatures = ABD \ [N; M];
epsilon0 = strains_curvatures(1:3);
kappa = strains_curvatures(4:6);

% Ply stresses/strains
```

```
fprintf('Optimal Laminate: [0/45/-45/90/-45/45/0]\n');
for k = 1:length(angles)
    theta = angles(k);
    z = -7*t_ply/2 + (k-0.5)*t_ply;
    epsilon_global = epsilon0 + z*kappa;
    c = cosd(theta); s = sind(theta);
    T = [c^2, s^2, 2*c*s; s^2, c^2, -2*c*s; -c*s, c*s, c^2-s^2];
    Qbar = inv(T) * Q * inv(T)';
    sigma_global = Qbar * epsilon_global;
    sigma_local = T * sigma_global;

    % Tsai-Wu index
    F11 = 1/(S1t*S1c); F22 = 1/(S2t*S2c); F66 = 1/T12^2;
    F1 = 1/S1t - 1/S1c; F2 = 1/S2t - 1/S2c; F12 = -0.5/sqrt(S1t*S1c*S2t*S2c);
    FI = F11*sigma_local(1)^2 + F22*sigma_local(2)^2 + F66*sigma_local(3)^2 + ...
        2*F12*sigma_local(1)*sigma_local(2) + F1*sigma_local(1) + F2*sigma_local(2);

% Compute local and global strains
fprintf('\n--- Strain Analysis ---\n');
for k = 1:length(angles)
    theta = angles(k);
    z = -7*t_ply/2 + (k-0.5)*t_ply;
    epsilon_global = epsilon0 + z*kappa; % Global strains
    c = cosd(theta); s = sind(theta);
    T = [c^2, s^2, 2*c*s; s^2, c^2, -2*c*s; -c*s, c*s, c^2-s^2];
    epsilon_local = T * epsilon_global; % Local strains

    fprintf('Ply %d: %d°\n', k, theta);
    fprintf('  Global Strains: εx = %.6f, εy = %.6f, γxy = %.6f\n', epsilon_global(1),
epsilon_global(2), epsilon_global(3));
    fprintf('  Local Strains: ε1 = %.6f, ε2 = %.6f, γ12 = %.6f\n\n', epsilon_local(1), epsilon_local(2),
epsilon_local(3));
end
```

CURRICULUM VITAES

Enes AKYOL

EDUCATION

2020 – 2026	**Marmara University – Istanbul, Turkey** Mechanical Engineering Department (4+1 Years Programme)
2020	**Rami Atatürk High School – Istanbul, Turkey**

EXTRA CURRICULAR ACTIVITIES

Mar 2025 – Mar 2025	ISKUR – Education of ISG

SKILLS

Language	Turkish (Native), English (Intermediate), German (Beginner)
Computer Skills	Microsoft Office Programs (Advanced), AutoCAD, MATLAB, SolidWorks, Python, LTspice
Hobbies	Volleyball, Skating, Travelling, Reading, Drawing

Amirmohammad MOTTAGHINIA

EDUCATION

2020-2026 **Marmara University- Istanbul, Turkey**
Mechanical Engineering Department

2020 **Shahed High School - Urmia, Iran**

SKILLS

Language	English, Turkish, Persian
Computer Skills	Word- Excel -PowerPoint

Rikesh POKHAREL

2021 – Present : MARMARA UNIVERSITY – Istanbul, Turkey. CGPA - 3.15/4.00

2019 : Little Angels CIE A Levels College - Kathmandu, Nepal

PERSONAL STATEMENT

My love of strategic games like chess and sudoku reflects my lifelong fascination with problem-solving. Because of my curiosity, I decided to pursue a degree in mechanical engineering, where I still study the principles and mechanics about how things operate. Understanding, designing, and improving systems converting theoretical knowledge into workable solutions is what motivates me.

EXPERIENCE

Summer Engineering Intern – ASELSAN (a'gelecek programı)

(Aug 2024 – Sep 2024 | Akyurt, Ankara, Türkiye)

Department: Mikroelektronik Güdüm ve Elektro-Optik Sektör Başkanlığı (MEGO)

(Microelectronics, Guidance, and Electric-Optics Sector)

Work Department: Makine Tasarim Müdürlüğü (MTM)

Work Title: Mechanical Design Intern

- Worked on the mechanical design of MGEO systems with gimbal mechanisms.
- Focused on vibration analysis, infrared system integration, and thermal management (heating and cooling) within MGEO systems.

Language : English (IELTS 8.0), Turkish (Tömer C1) , Nepalese,

Computer Skills : PTC CREO, SOLIDWORKS, AUTOCAD, MATLAB, MS OFFICE,

Hobbies : Chess, football, problem solving quizzes, traveling